British Geological Survey

Understanding the relationship between groundwater chemistry and corrosion for rural water supplies

Groundwater Programme

Open Report OR/26/057

BRITISH GEOLOGICAL SURVEY

GROUNDWATER PROGRAMME

OPEN REPORT OR/26/057

Keywords

Report; corrosion, groundwater, statistics

Front cover

Corroded components from an India Mark II handpump.

Bibliographical reference

MacAllister, D J, Smedley, P L, and Arran, M. 2026. Understanding the relationship between groundwater chemistry and corrosion for rural water supplies. *British Geological Survey, Open Report OR/26/057*. 34 pp.

Understanding the relationship between groundwater chemistry and corrosion for rural water supplies

DJ MacAllister, P L Smedley, M Arran

Editor

J M Hannaford

Keyworth, Nottingham British Geological Survey 2026

BRITISH GEOLOGICAL SURVEY

The full range of our publications is available from the BGS online shop https://shop.bgs.ac.uk/ and our Cardiff office (Welsh publications only). The London Information Office also maintains a reference collection of BGS publications, including fossils, for consultation.

We publish an annual catalogue of our maps and other publications; this catalogue is also available online.

The British Geological Survey carries out the geological survey of Great Britain and Northern Ireland (the latter as an agency service for the government of Northern Ireland), and of the surrounding continental shelf, as well as basic research projects. It also undertakes programmes of technical aid in geology in developing countries.

The British Geological Survey is a component body of UK Research and Innovation.

British Geological Survey offices

Nicker Hill, Keyworth,
Nottingham NG12 5GG
Tel 0115 936 3100

BGS Central Enquiries Desk
Tel 0115 936 3143
email enquiries@bgs.ac.uk

BGS Sales
Tel 0115 936 3241
email sales@bgs.ac.uk

The Lyell Centre, Research Avenue South,
Edinburgh EH14 4AP
Tel 0131 667 1000
email scotsales@bgs.ac.uk

Natural History Museum, Cromwell Road,
London SW7 5BD
Tel 020 7589 4090
Tel 020 7942 5344/45
email bgslondonstaff@bgs.ac.uk

Cardiff University, Main Building, Park Place,
Cardiff CF10 3AT
Tel 029 2167 4280

Geological Survey of Northern Ireland, 7th Floor,
Adelaide House, 39-49 Adelaide Street, Belfast, BT2 8FD
Tel 0289 038 8462
www2.bgs.ac.uk/gsni/

Natural Environment Research Council, Polaris House,
North Star Avenue, Swindon SN2 1EU
Tel 01793 411500 Fax 01793 411501
www.nerc.ac.uk

UK Research and Innovation, Polaris House,
Swindon SN2 1FL
Tel 01793 444000
www.ukri.org

Website: https://www.bgs.ac.uk
Shop online: https://shop.bgs.ac.uk/

Foreword

This report is the published product of a study by the British Geological Survey (BGS) using groundwater and borehole corrosion data from study areas in Ethiopia, Malawi and Uganda, collected under the Hidden Crisis project, funded under the Natural Environment Research Council's UPGro research programme (2013 to 2020). The current study was carried out with the support of the Waterloo Foundation over the period November 2024 to March 2026.

Acknowledgements

Acknowledgement is due to Kerstin Danert (Ask for Water) for managing the wider Stop the Rot project and for discussions, advice and review of this report. We thank Alan MacDonald (BGS) for helpful discussions and support throughout, particularly sharing his insight into the data collected during Survey 1. Thanks are due to Jenny Bearcock for reviewing the report. We thank the Waterloo Foundation for funding this work (Grant reference number: 1730/7660). The work builds on, and uses data from, the Hidden Crisis project which was part of the Natural Environment Research Council (NERC), UK Foreign, Commonwealth and Development Office (FCDO), and Economic and Social Research Council (ESRC) funded research programme Unlocking the Potential of Groundwater for the Poor (UPGro) (grant number NE/M008606/1). Additional financial support was provided by the NERC-UKRI ODA- National Capability Foundation Award (NE/R000069/1) and the NERC National Capability Science International Award (NE/X006255/1).

Contents

FIGURES

TABLES

Executive summary

Corrosion of handpumps has been a persistent problem in sub-Saharan Africa and has been documented for at least forty years. Corrosion can impact hand-pump functionality and contaminate water supplies. The rate and severity of corrosion is controlled by groundwater chemistry as well as the type and quality of metal pump components.

A range of indicators has been used to assess the risk of corrosion of metallic components of handpumps installed in groundwater. The Larson-Skold index, the Langelier Saturation index and the Ryznar Stability index are the most commonly used indicators. These indices assess different aspects of the corrosivity of groundwater. The Langelier and Ryznar indices examine the effects of pH, temperature, calcium concentration, alkalinity and salinity; the Larson-Skold index accounts for the influence of the corrosive ions sulphate and chloride in relation to alkalinity.

The simplest indicator used to assess the risk of corrosion is pH. Observational evidence from sub-Saharan Africa by Otto Langenegger in the late 1980s and early 1990s was used to conclude that, where the pH of groundwater is less than 6.5, galvanised iron or mild steel should not be installed. However, for the next forty years, these materials continued to be installed and the problem of corrosion proliferated. To date, corrosion of hand-pumps has been documented in at least 20 countries across sub-Saharan Africa.

The aim of this study, undertaken as part of the ‘Stop the Rot’ initiative, was to characterise the corrosivity of the groundwater chemistry and to predict the probability of corrosion and leaching of corrosion by-products into the groundwater, using existing data from the Hidden Crisis project. The Hidden Crisis project took place between 2016 and 2019 in Ethiopia, Malawi and Uganda and was an interdisciplinary project designed to examine the physical, technical and social determinants of hand-pumped borehole functionality across two surveys. Water samples were collected and analysed across both surveys.

Interpretation of water-chemistry data and corrosion indices shows that:

- most groundwater from the sites sampled had a tendency towards corrosivity, as indicated by the corrosion indices
- pH values of less than 7 were common in the dataset, further indicating that groundwater at the study sites was corrosive
- elevated concentrations of iron, manganese and lead can be associated with corrosion but, in the Hidden Crisis dataset, these appear to be derived largely from the aquifer rather than the hand-pump
- chromium, cadmium and zinc may be associated with hand-pump corrosion

Statistical models were constructed to predict the likelihood of corrosion based on the water chemistry results and using the observations of corrosion made during the Hidden Crisis project. The statistical models showed that:

- the most effective predictive models of corrosion for galvanised iron rising mains and rods use the full water chemistry dataset; however, such models are challenging to interpret, especially as the water chemistry parameters that are important in these models vary significantly between component type
- pH below 6.5 is the most effective binary indicator of corrosion for galvanised iron components:
    - for galvanised iron rising mains:
        - the corrosion probability is 61 % if pH is less than 6.5
        - the corrosion probability is 30 % if pH is greater than 6.5;
    - for galvanised iron rods:
        - the corrosion probability is 61 % if pH is less than 6.5
        - the corrosion probability is 50 % if pH is greater than 6.5;

- corrosion can still occur when pH is neutral or alkaline; in these cases, corrosion indices and more comprehensive assessments of water chemistry are required

Based on these results, we recommend that:

- comprehensive assessment of major-ion water chemistry should be conducted as a default where budgets allow and when galvanised iron is intended to be replaced by stainless steel
- where budgets are more limited, the use of pH thresholds can provide a useful indicator of the risk of corrosion
- pH must be measured accurately using well maintained and regularly calibrated pH sensors
- any galvanised metalwork used for groundwater installations should be in accordance with recommended manufacturing guidelines
- galvanised iron components should not be installed in groundwater with a pH of less than 6.5
- where pH is over 6.5, an assessment of the wider tendency of groundwater to be corrosive should be made using corrosion indices
- at a minimum, groundwater chemical analysis should investigate the following parameters:
    - pH
    - temperature
    - major ions: calcium, magnesium, sodium, potassium, chloride, sulphate and nitrate

Better monitoring and preventative maintenance of rural water infrastructure can reduce the impact of corrosive groundwater on handpump condition and functionality:

- replacement of galvanised iron components with corrosion-resistant alternatives
- regular monitoring of condition of downhole components
- replacement of parts at regular intervals (as recommended in the hand-pump user manuals)
- adherence to standards as laid out in international and national specifications

1 Introduction

Corrosion of handpumps in sub-Saharan Africa (SSA) is a well-known phenomenon and has been reported since the 1980s (Langenegger, 1989, 1994; Clarke, 1980). Handpump corrosion has been documented in at least 20 SSA countries (Danert, 2022). Corrosion can impact the functionality of handpumps (MacAllister et al., 2022), resulting in failure and long periods of downtime, as well as impacting the quality of water drawn from the handpump (Casey et al., 2016). Iron contamination is a particular problem that has been well documented across SSA (Casey et al., 2016) but leaching of other contaminants, including lead (Pb), has also been associated with corrosion (Fisher et al., 2021; Rezek et al., 2026).

The rate and severity of corrosion is influenced by groundwater chemistry. This project assessed the tendency for corrosion of metallic groundwater infrastructure (handpumps) and the groundwater scaling potential, the latter of which can retard the rate of corrosion.

1.1 CORROSION AND SCALING MECHANISMS

Metal corrosion occurs by electrochemical redox reactions as the metal structure trends towards a return to its natural oxidised state. A potential difference is set up between one section of corroding metal and another, with a transfer of electrons between the corroding surface (anode) and the non-corroding surface (cathode) in the presence of an electrolyte solution. Metallic iron (Fe) corrodes in the presence of the electrolyte and oxygen (O_2) to produce an oxidised rust of iron hydroxide ($Fe(OH)_3$), which may partially coat the corroded metal surface. Oxidation of the metal occurs at the anode and reduction, usually of O_2, at the cathode. Electrochemical cells can be set up by spatial differences in metal composition, surface coating compositions, contact of different metals or varying electrolyte composition (Benefield et al., 1982).

Galvanic corrosion occurs when metals of dissimilar electrical potential are in contact in the presence of an electrolyte. The more reactive metal that forms the anode corrodes preferentially, while the cathode is protected. The more dissimilar the two metals, the more pronounced the corrosion. Galvanised iron or steel can be particularly prone to corrosion when joined to dissimilar metals such as copper (Cu) (World Health Organization, 2022). Galvanised metal can release zinc (Zn) as well as cadmium (Cd) and Pb from the surface galvanising layer. Stainless steel with a minimum of 11 % chromium (Cr) is more resistant to corrosion. A passive surface layer of Cr oxide protects the underlying steel.

Alloying metals such as Cr, nickel (Ni), molybdenum (Mo) and Cu added to steel help to harden and improve resistance to corrosion. These form a surface oxide coating. Stainless steel is relatively resistant but, where oxide coated, can be prone to pitting corrosion or the localised dissolution of the metal caused by the breakdown of the normally passivating surface layer. The effects depend on factors such as temperature, solution composition and redox environment, as well as the composition of the steel itself. Pitting corrosion is commonly associated with chloride (Cl)-bearing solutions; pits can be highly corrosive microenvironments resulting from the local build-up of hydrochloric acid (HCl) (Ma, 2012). Further isolation of the pits can result from local surface deposition of corrosion products (such as $Fe(OH)_3$), with resulting further corrosion. Pitting corrosion is also favoured in poorly oxygenated environments where further formation of protective surface metal oxide is inhibited (Ma, 2012).

Corrosion can be exacerbated by solutes including Cl and SO_4; brackish water is more corrosive than fresh water. Other corrosive solutes include dissolved carbon dioxide (CO_2) and sulphide (including H_2S). Generation of H_2S may be caused or facilitated by microbial activity.

Scaling is the production of mineral coating on infrastructure including metal surfaces, usually by mineral precipitation but sometimes used in the context of deposits of secondary metal oxides produced by the corrosion of metal. Scaling most commonly involves calcite as well as oxides of Fe and aluminium (Al). In some cases, scaling can provide a protective layer and inhibit the rate and extent of corrosion.

1.2 CORROSION INDICES

Several corrosion indices exist (Roberge, 2007) and have been used to predict the corrosivity of groundwater (Mankikar, 2021, Robinson, 2024, Eslami et al., 2020). The most used indices are the Langelier saturation index (LSI), the Ryznar stability index (RSI) and the Larson-Skold index (LSkI):

- LSI and RSI examine the effects of pH, calcium (Ca) concentration, alkalinity and salinity on groundwater corrosivity; they are used to predict whether a protective layer of calcium carbonate ($CaCO_3$) will form on the pipe surface
- LSkI accounts for the influence of the corrosive ions SO_4 and Cl in relation to alkalinity

However, these indices are rarely used in the rural supply sector, and many use a pH threshold as the primary indicator of corrosion risk. Following extensive experimentation and field testing of handpump components, Langenegger (1989) first proposed the use of threshold of pH less than 6.5 as an effective indicator of corrosion risk for rural handpumped boreholes using galvanised iron rising mains and rods. More recently, the World Bank (2024) has advocated that countries use this threshold when assessing the risk of handpump corrosion.

1.3 HANDPUMP FUNCTIONALITY AND CORROSION

An investigation of borehole functionality, including impacts of metal corrosion on borehole infrastructure and of microbial and chemical quality of groundwater, was carried out in three SSA countries. The NERC/FCDO/ESRC-funded project ‘Hidden Crisis: unravelling current failures for future success in rural groundwater supply’ aimed to understand the underlying reasons for poor functionality of handpumped boreholes in Ethiopia, Uganda and Malawi. Functionality of rural water supplies in these three African countries has been a persistent issue. The three countries use two different types of handpumps: India Mark II handpumps are used in Ethiopia and Uganda and the Afridev is used in Ethiopia and Malawi. Occasionally, the India Mark II deep well and India Mark III variants are used in Uganda and Ethiopia. For clarity, all India Mark handpump variants will be collectively referred to as India Mark handpumps.

The Afridev is designed to be maintained by communities and uses corrosion-resistant materials. India Mark handpumps use galvanised iron rising mains and requires more expertise to repair.

The Hidden Crisis project examined the physical, technical and social determinants of handpumped borehole functionality across two surveys. In the first survey of the project, 200 handpumped boreholes were selected in each country using a stratified random sampling approach. Then, using a nuanced definition of functionality (Bonsor et al., 2018), each handpump borehole was classified as one of six functionality categories:

- fully functional
- partially functional with low yield
- partially functional with poor reliability
- partially functional with both poor yield and reliability
- non-functional
- abandoned

These classifications were made based on a simple handpump stroke test and a questionnaire about the performance of the handpump in the last year. In the first survey of the Hidden Crisis project, where a comprehensive suite of water-quality parameters was measured (Lapworth et al., 2020), samples were collected by manually pumping the handpump. Since samples were collected with the handpump in situ, this theoretically allowed an assessment of the influence of the handpump on groundwater quality.

The second survey of the Hidden Crisis project involved a more comprehensive assessment of the underlying reasons for the functionality status of a subset of handpumped boreholes surveyed in the first survey. Up to 50 handpumped boreholes were selected in each country, based on the functionality categorisation determined in the first survey. Up to 10 handpumped boreholes in each functionality category were purposively selected for more detailed investigations. These more detailed investigations involved dismantling and removing the

handpump from the borehole and conducting pumping tests, borehole CCTV surveys, detailed qualitative and quantitative observations of component condition and further water-quality testing at each site. Water-quality sampling in the second survey was conducted after pumping the borehole for at least two hours, theoretically allowing assessment of the natural aquifer water quality without interference from the handpump. This second survey also allowed a detailed assessment of the physical, technical and social determinants of handpump borehole functionality (MacAllister et al., 2022, 2026). However, corrosion risk and impacts were not systematically investigated during the Hidden Crisis project. Thus, there was an opportunity to examine corrosion mechanisms in more detail as part of the Stop the Rot initiative.

1.4 AIMS AND OBJECTIVES

The aim of the study was to characterise the corrosivity of the groundwater chemistry and to predict the probability of corrosion and leaching of corrosion by-products into the groundwater. Using the Hidden Crisis project surveys 1 and 2 water chemistry datasets, the objectives were to:

- interpret and characterise groundwater geochemistry with reference to corrosivity
- calculate corrosion and mineral saturation indices based on the groundwater geochemistry
- use measurements of water chemistry, corrosion indices and observations of handpump corrosion to predict the probability of corrosion and determine which water quality parameters have the greatest predictive power
- predict the probability of groundwater contamination based on the observed extent of corrosion of handpump components

2 Observations of corrosion

During the Hidden Crisis project, corrosion of handpump components was assessed using systematic field-based observations (some examples of which are provided in Figure 1). In addition, galvanising and pipe-wall thickness measurements were made. The methodology for assessing corrosion and measuring thicknesses is described in section 3.1.2 of the report. Results of these observations and measurements are presented in MacAllister et al. (2022) and only a summary is provided here (Table 1).

In Uganda, 61% of rising main pipe sections were corroded and 82% of pump rods were corroded. In Ethiopia, 37% of rising main pipes and 55% of pump rods were corroded. In Malawi, where non-corrosive PVC pipes are used, 43% of pump rods were corroded. Galvanising thicknesses on rising main pipe sections were below standards (65 µm) in 75% of pipe in Ethiopia and 98% in Uganda. Pipe wall thicknesses were below standards (3.25 mm) in 93% of sites in Ethiopia and 67% in Uganda. Pipe wall thicknesses for Afridev handpumps were below standard thicknesses (4.7 mm) in 20% of sites in Malawi and 52% of sites in Ethiopia.

Table 1 Proportions of corroded hand-pump pipes corroded by country. Data from MacAllister et al., 2022.

Country	% rising main pipes corroded	% pump rods corroded	% galvanising thickness below standard	% pipe-wall thickness below standard	% pipe-wall thickness below standard (Afridev)
Ethiopia	37	55	75	93	52
Malawi	-*	43	-	-	20
Uganda	61	82	98	67	-

* PVC pipes used

The observations of corrosion and quantitative measurements of galvanising and pipe-wall thickness illustrate the extent of the corrosion problem in the three study countries. Uganda has significant and widespread issues with corrosion. The aim of this work was to gain a better understanding of how water chemistry might explain these observations and to provide a quantitative assessment of its role.

(a)

(b)

(c)

(d)

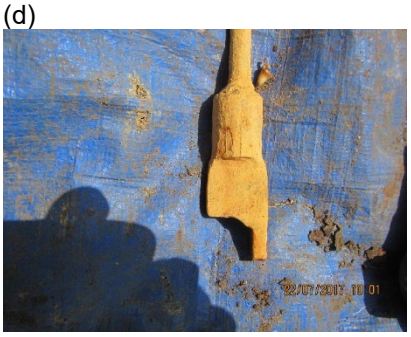

(e)

(f)

(g)

(h)

Figure 1 Observations of corrosion of handpump components made during the Hidden Crisis project in Ethiopia and Uganda. All photographs are of India Mark handpump components. (a) to (e) Corroded rod sections; (f) and (g) corroded rising main sections; (h) corroded cylinder. BGS © UKRI 2026.

3 Method

3.1 DATASETS

3.1.1 Groundwater quality dataset

The study used previous groundwater data collected by BGS and partners as part of the NERC UPGro Hidden Crisis project, which was conducted over the period 2016 to 2019. Groundwater samples were collected from rural water supply handpumped boreholes in Ethiopia, Malawi and Uganda in terrain dominated by crystalline basement, consolidated sediments, unconsolidated sediments or volcanic rocks.

Borehole depth ranges were (MacAllister et al., 2022):

- Ethiopia: 18.7 to 84.3 metres below ground level (mbgl)
- Malawi: 14.7 to 65.8 mbgl
- Uganda: 26.7 to 101 mbgl

Sampling and field analysis in each country was carried out by local teams in two surveys, the first in 2016 and the second in 2017 and 2018. Sampling spanned the seasons:

- Survey 1:
    - Ethiopia: April to June 2016
    - Malawi: September to December 2016
    - Uganda: July to September 2016
- Survey 2:
    - Ethiopia: April to August 2017
    - Malawi: September to March
    - Uganda: June to November 2017

Survey 1 involved manually pumping groundwater directly from the handpump for 30 minutes before completion of tests, including water sampling. Survey 2 involved sampling at the end of 2.5-hour pumping tests after removal of the handpump and insertion of a submersible pump in the borehole. During Survey 2, pumping test unstable parameters (redox potential (Eh); dissolved O (DO); temperature) were monitored for 30 minutes before reporting measurements and collecting samples.

All field and local analytical measurements were made on unfiltered samples; samples collected for subsequent laboratory analysis were filtered to 0.45 µm and samples for analysis of major cations and trace metals were acidified (to 1% v/v HNO_3).

- Survey 1 included chemical analyses of a total of 428 samples
- Survey 2 included analysis of 141 samples

The first survey was more comprehensive spatially but included fewer analytes (47 chemical and physicochemical analytes in Survey 1; 75 in Survey 2 (Appendix 1)). The second survey involved detailed borehole survey (condition of borehole and pump components), pump testing and chemical analysis.

Laboratory analysis for Survey 1 was conducted by Flinders University (CSIRO) by ion chromatography, ICP-OES and ICP-MS (Lapworth et al., 2020). Sample analysis for Survey 2 was carried out by BGS using ion chromatography and ICP-MS. Analytes and respective detection limits were different between the two surveys.

For the current study, we used available laboratory chemistry data from Survey 1, along with field chemistry data. For Survey 2, we used:

- borehole metadata
- field and laboratory chemistry data
- manually measured water levels from pumping tests
- descriptions of the condition and dimensions of pump components, rising mains and rods

The fields in the datasets required standardisation in the recording of missing values, Boolean variables and spelling.

Even with standardisation, the dataset required certain values to be populated using alternative measurements from other columns, negative Fe concentrations in Survey 1 to be zeroed and concentrations censored by measurement limits (measurements below analytical detection limits) to be infilled. Such values were populated, where possible, by maximum-likelihood estimation of the parameters of an assumed underlying lognormal distribution, given available measured concentrations. If more than half of available measurements for a particular parameter were censored (below detection limit) but all uncensored measurements were above detection limits, then concentrations below detection limits were taken to be zero. However, if any measured value was below detection limit, then values were taken to be missing.

3.1.2 Corrosion dataset

All components of each handpump were photographed (for example, Figure 1) and visual observations of condition were made. The condition of components was classified based on a list of three predefined condition categories:

- corroded: visible surfaces with (Langenegger, 1989, 1994; Clarke, 1980):
    - precipitate or scaling
    - red or orange staining
    - pitting
    - flaky or powdery surface texture
- damaged:
    - bent
    - cracked
    - dented
    - worn
- missing

Measurements were made of rising main galvanising thickness using an Elcometer® 456 coating thickness gauge and magnetic probe with an accuracy of ±2.5 µm and resolution of 0.1 µm. Pipe wall thickness was measured using an Elcometer® MTG4 ultrasonic material thickness gauge and a 1 MHz transducer for galvanised iron pipes (India Mark) and a 5 MHz transducer for PVC pipes (Afridev), both with an accuracy and resolution of ±0.1 mm.

3.2 CHEMISTRY DATA QUALITY ASSURANCE

The analytical data from the two surveys has been used together for the assessment of the corrosion or scaling potential of the collected groundwaters and continues from previous investigations (MacAllister et al., 2022). Indicators of corrosion or scaling potential and geochemical models to assess groundwater quality and potential impacts rely on carbonate equilibria and incorporate values for alkalinity, total dissolved solids (TDS), pH and Eh. Hence, establishing these parameters as accurately and precisely as reasonably possible was considered an important first step.

The Hidden Crisis data downloaded from a Microsoft Access table was firstly assessed for analytical quality. Complete analyses of major ions were available for each sample and charge balances were calculated from the analytes for each survey. Charge balance is a check on whether the total positive and negative ionic charges in a water sample are approximately equal, indicating chemically consistent analytical results. One of the largest areas for potential discrepancy is with field-titrated total alkalinity (Figure 2).

3.2.1 Total alkalinity

Total alkalinity measurements were made at the time of sampling by the local field teams, using a Hach digital titrator against 1.6N sulphuric acid (H_2SO_4) or (less commonly) 0.16N H_2SO_4. Measurements were replicated two or three times until at least two results matched within 10 %, then the average was usually taken as the final measurement. Measurements were in almost all cases made on samples of 50 mL. All alkalinity measurements were converted to bicarbonate

(HCO_3) in the original datasets and are reported as such in this report. Charge balances for both surveys are shown in Figure 2a and Figure 2b as received.

Field data sheets were checked for accuracy of total alkalinity data transfer. Most samples were found to be recorded correctly but some replicates showed poor reproducibility. Where more than two replicates were recorded and one was appreciably different (over 10 %), the more consistent measurements were averaged. In some cases, earlier charge imbalances had clearly resulted in re-tests of total alkalinity by acid titration in the laboratory. These had not always been adopted as the preferred values in the original database but, where available, they were used here.

3.2.2 Charge balance

Figure 2 shows a comparison of the distributions of charge balances from the two surveys, before (a and b) and after (c and d) the alkalinity and balance assessments and corrections. After cleaning, a large proportion of samples retain poor charge balances (41 % greater than 5 % imbalanced for Survey 1 and 35 % for Survey 2). No replicates or blanks were present in the database to check the data quality further. Subsequent use of analytical data was restricted to analyses with balances within ±10 %. This restricted the size of dataset available for the investigation but ensured greater confidence in the selected data.

TDS values were calculated for this investigation according to APHA method 1030 E (APHA, 2021) using laboratory chemical data, following standard practice. Oxidation-reduction potential (ORP) values were analysed and reported only for Survey 2 samples. These values were converted to Eh (corrected to the standard hydrogen electrode) for the current project.

3.2.3 Total and dissolved iron

In both surveys, total Fe was measured on unfiltered samples by colorimetry using a Hach DR300 pocket colorimeter with TPTZ (2,4,6-Tris(2-pyridyl)-s-triazine) powder pillows (0.04 to 1.8 mg/L measurement range). The reagent, which includes a reducing agent and pH buffer, reduces ferric Fe and complexes ferrous Fe. For total Fe including particulates, an extra digestion step is recommended first, to ensure any particulate Fe is fully represented. Therefore, the measured total Fe concentrations may not be fully representative of all forms of Fe present in the samples.

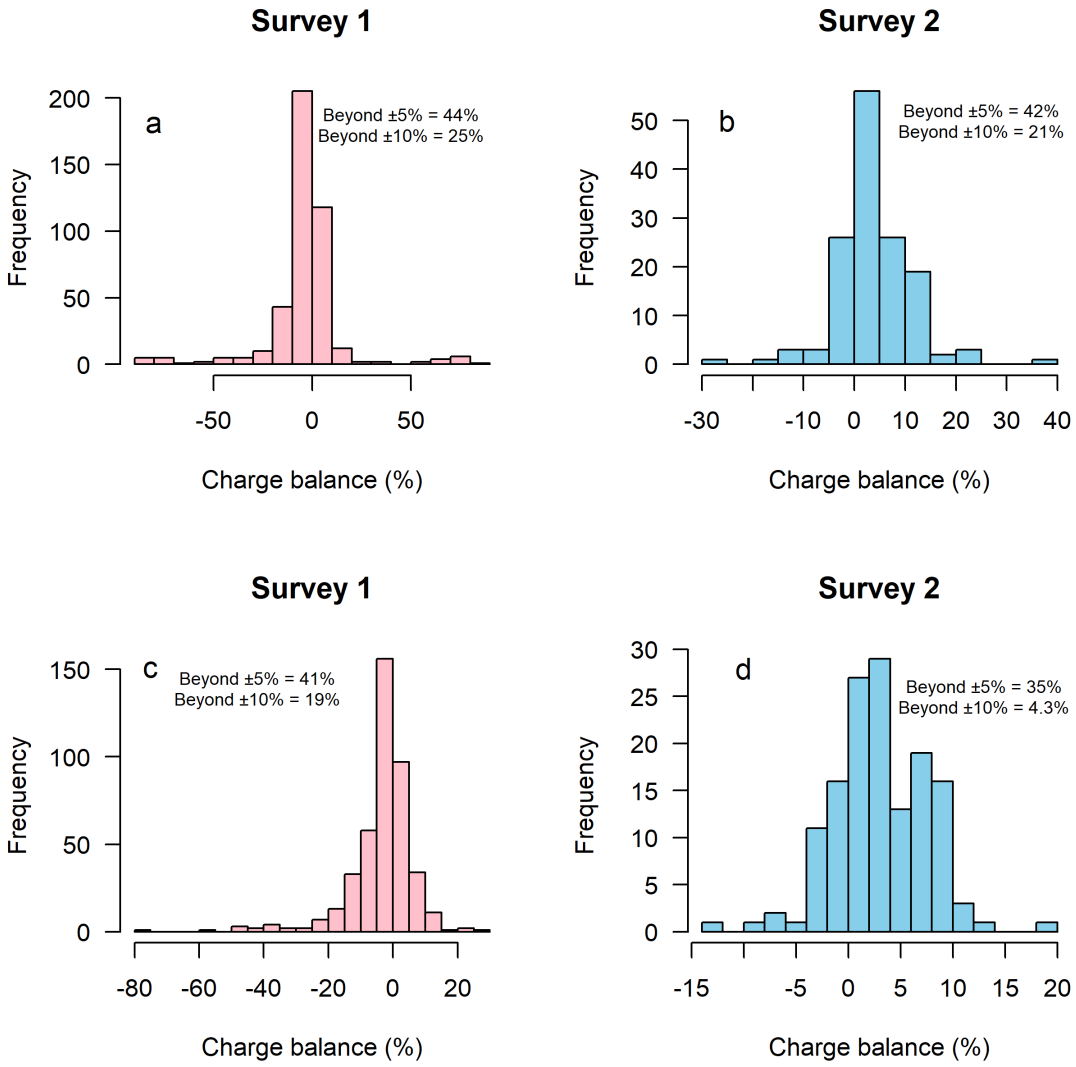

Figure 2 Charge balances for water samples collected in surveys 1 and 2. a and b: as received; c and d: following checks and corrections to analytical data. BGS © UKRI 2026.

Total Fe (unfiltered; colorimetry) showed little relation with dissolved Fe (laboratory) in either survey (Figure 3a). Samples with highest concentrations of total Fe correspond with those with highest concentrations of dissolved Fe in Survey 2, but the concentration ranges differed, the former reaching an observed maximum around 2 mg/L.

Laboratory measurement of dissolved Fe (in filtered samples) was by ICP-OES in Survey 1 and ICP-MS in Survey 2. Detection limits were typically two orders of magnitude different between the two surveys (100 µg/L in Survey 1; 5 µg/L in Survey 2).

3.2.4 Turbidity

Turbidity, a measure of the cloudiness of water, was determined by optical scattering using a field turbidimeter. Water samples were collected in a glass vial with screw-top lid and placed in the device.

Turbidity might be expected to show some correlation with total Fe as particulate Fe is commonly a component of cloudy water. Total Fe does show some relationship with turbidity in Survey 1 but, as noted previously, the relationship was affected by the apparently suppressed total Fe values in Survey 2 (Figure 3b).

Highest total Fe, dissolved Fe and turbidity values are most commonly observed in groundwater from Uganda, with some high turbidity values (>100 NTU) from Malawi (Figure 4b).

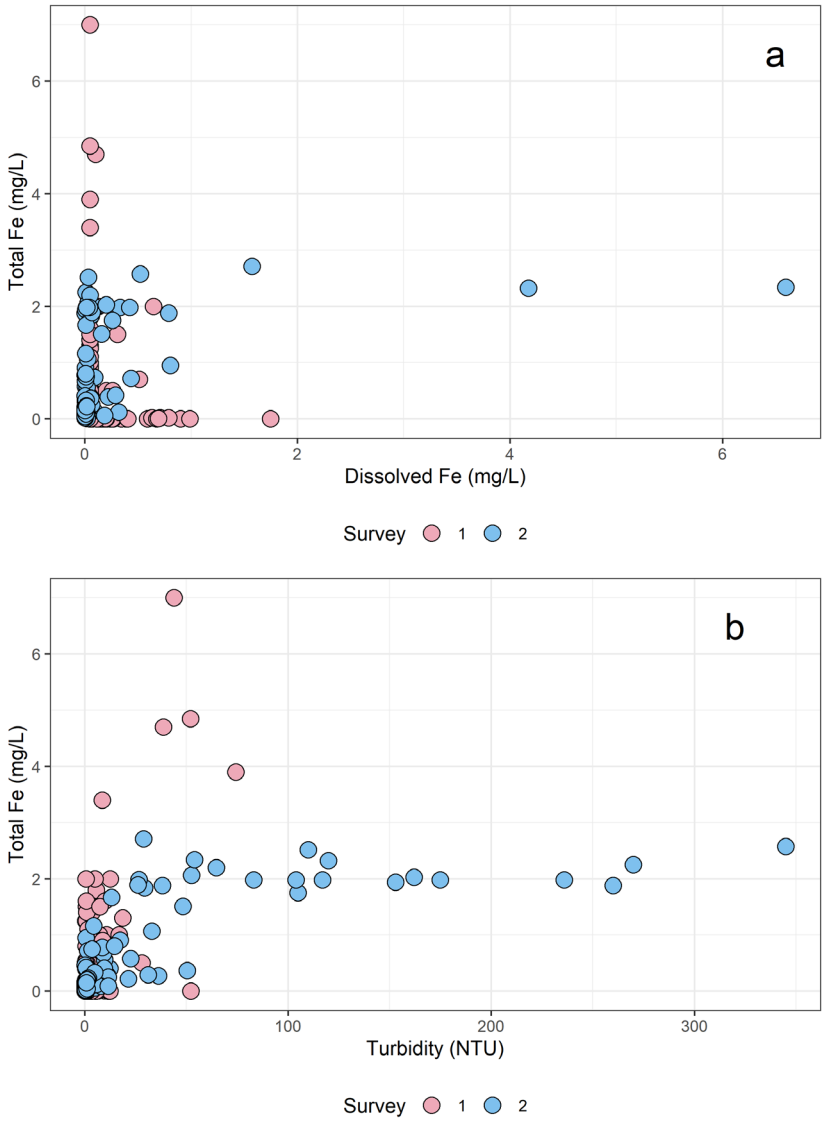

Figure 3 a) total Fe (unfiltered, by colorimetry) against dissolved Fe; b) total Fe against turbidity for groundwater samples from surveys 1 and 2 (with charge balances better than ±10 %). BGS © UKRI 2026.

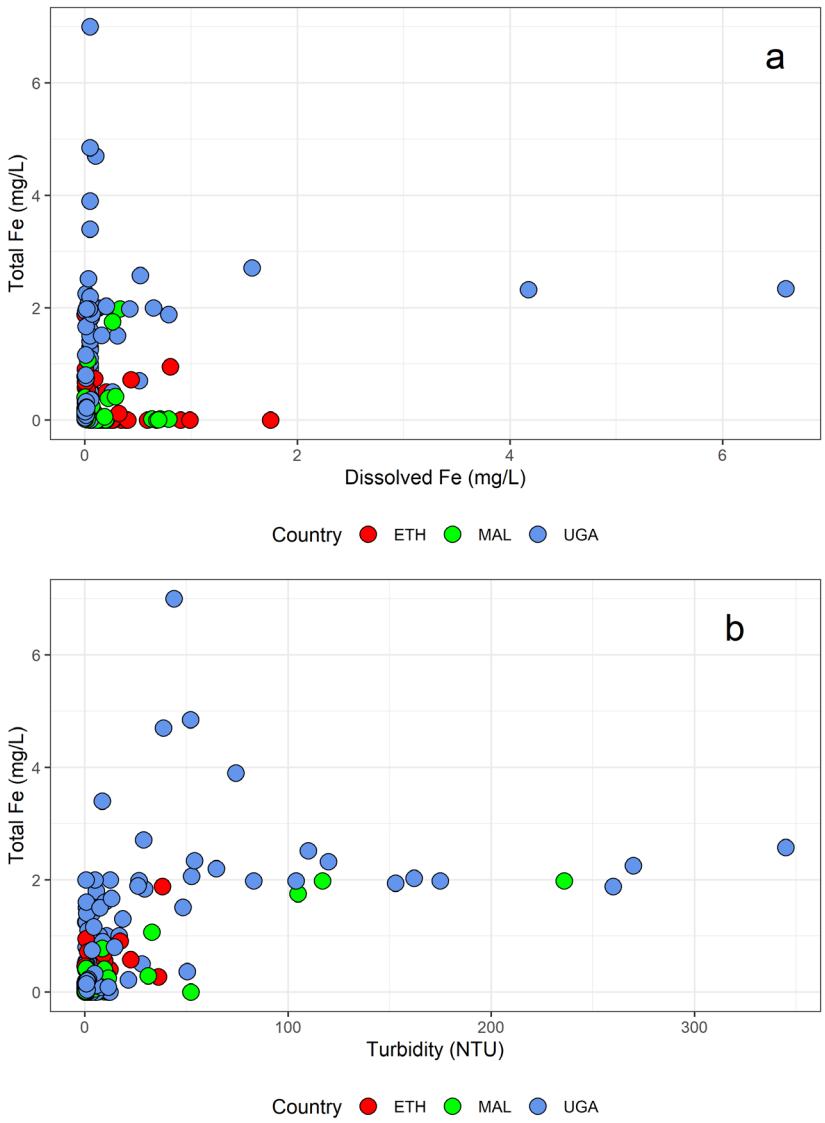

Figure 4 a) total Fe against dissolved Fe; b) total Fe against turbidity, distinguished by country. BGS © UKRI 2026.

3.2.5 Metal analysis

Laboratory analyses of metals relied on groundwater samples filtered to 0.45 µm. This allows potential particulate and colloidal matter through the membrane filter below that dimension and could contribute to the load of metals determined as dissolved. No analyses from samples filtered with finer mesh were available in the database to compare for assessing the fine particulate and colloidal fraction.

3.2.6 pH

The variability in pH measurements for sites sampled during both surveys is shown in Figure 5. The correlation is relatively weak. This may reflect true temporal variation between sampling campaigns, but measurement uncertainty is also a possible factor and needs to be borne in mind when interpreting and using pH measurements.

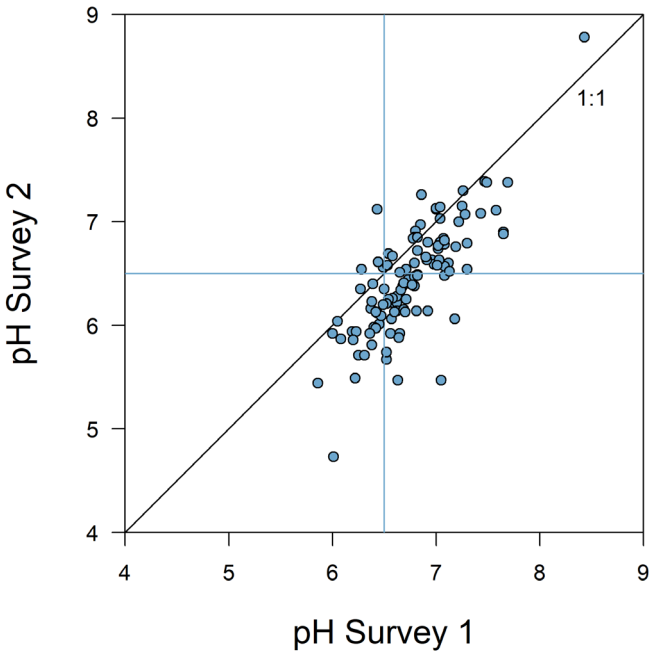

Figure 5 Variation in pH values between surveys 1 and 2; plot shows the pH 6.5 threshold for each survey and the 1:1 line. BGS © UKRI 2026.

3.3 CALCULATING SATURATION AND CORROSION INDICES

Data from groundwater samples from both surveys 1 and 2 were used to calculate corrosion indices and the calcite saturation index ($SI_{calcite}$). All indices follow similar principles and aim to assess the tendency for precipitation of either calcite scale or to be aggressive with a greater potential for metal corrosion.

3.3.1 Calcite saturation index

$SI_{calcite}$ is a measure of the condition of a given solution with respect to calcite equilibrium and is determined by the ratio of its ion activity product (IAP) to the calcite solubility product constant (K_{sp}). A ratio of 1 would suggest that the solution is at solubility equilibrium with calcite; if less, the solution is undersaturated and, if present, calcite should dissolve. If the ratio is greater than 1, the solution is oversaturated and calcite should precipitate. The saturation index is defined as the log of the ratio, so a solution in solubility equilibrium has an index of 0.

$$SI_{calcite} = \log_{10} \frac{IAP}{K_{sp}}$$

$SI_{calcite}$ is an indication of the tendency to dissolve or precipitate calcite in a solution and not a measure of the corrosivity of metal in the solution. However, a water that is oversaturated with respect to calcite will be prone to scaling due to calcite precipitation, the degree of scaling increasing with increasing degree of oversaturation. Scales can coat metal surfaces and may form a protective layer to limit metal corrosion. By association, water undersaturated with calcite (with low pH and potentially high pCO_2 values) may be more corrosive to metals.

Values for the $SI_{calcite}$ in each groundwater sample were calculated using PHREEQC v 3 (Parkhurst and Appelo, 2013) with the `phreeqc.dat` database.

3.3.2 Langelier saturation index

LSI is an empirical simplification closely related to $SI_{calcite}$ and has become probably the most widely used proxy indicator of metal corrosion in water-supply applications (Roberge, 2007). LSI is calculated from the solution's:

- alkalinity (mg/L as $CaCO_3$)
- Ca hardness (mg/L Ca as $CaCO_3$)
- TDS (mg/L)
- pH
- temperature (°C)

LSI is defined as the difference between measured pH and the pH at saturation with respect to calcite:

$$LSI = pH - pH_s$$

Where pH is the measured pH and pH_s is the pH at saturation:

$$pH_s = (9.3 + A + B) - (C + D)$$

Where:

$$A = \frac{(\log_{10}[TDS] - 1)}{10}$$

$$B = -13.12 \times \log_{10}(°C + 273) + 34.55$$

$$C = \log_{10}[Ca^{2+}\ as\ CaCO_3] - 0.4$$

$$D = \log_{10}[alkalinity\ as\ CaCO_3]$$

As for the $SI_{calcite}$, a negative LSI indicates calcite should dissolve if present; a positive LSI suggests calcite should precipitate, and an LSI of 0 indicates a solution in equilibrium with respect to calcite. The index can indicate a tendency to be corrosive to metals but is generally a less effective indicator of corrosion where extremes of pH, low alkalinity or Ca concentration and high concentrations of other potentially corrosive solutes such as Cl and SO_4 apply. In such solutions, Ca and Mg can form complexes and prevent protective surface scaling. The LSI is noted to be less applicable below alkalinity and Ca values of around 40 mg/L (each as $CaCO_3$) and beyond the pH range 6.5 to 9.5 (Benefield et al., 1982). LSI values were also calculated using variable activity coefficients (Benefield et al., 1982). These showed negligible difference from the method given here.

Comparison of the LSI data with data for $SI_{calcite}$ (Figure 6) shows a close correspondence around the calcite saturation point (down to about -0.5) but, at more undersaturated values, the slope diverges from a 1:1 relationship. The LSI records a greater degree of undersaturation. This is likely because PHREEQC models a fuller chemical speciation of the solutions, with greater differences in species represented in the model in strongly undersaturated, acidic (pH less than 6.5) samples.

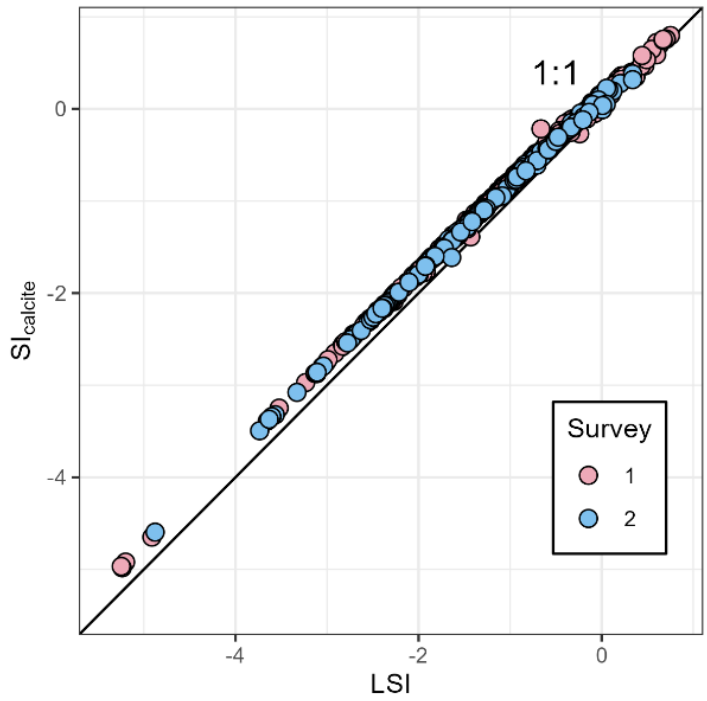

Figure 6 LSI against $SI_{calcite}$, arranged by survey. BGS © UKRI 2026.

3.3.3 Ryznar stability index

The related RSI focuses on the potential for scaling and is calculated using:

$$RSI = 2(pH_s) - pH$$

Where a value less than 6 indicates scaling tendency; more than 7 indicates little scaling, and more than 8 indicates potential for mild steel corrosion, the corrosion potential increasing with index value.

The Puckorius scaling index (PSI) uses a similar principle and the same pH_s, but incorporates equilibrium pH rather than measured pH:

$$PSI = 2(pH_s) - pH_{eq}$$

Where

$$pH_{eq} = 1.465 \times log_{10}[alkalinity] + 4.54$$

And

$$[alkalinity] = [HCO_3^-] + 2[CO_3^{2-}] + [OH^-]$$

A PSI greater than 6.5 indicates a tendency for corrosion and less than 4.5 a tendency for scale formation.

3.3.4 Larson-Skold Index

LSkI has been used to assess water corrosivity to mild steel and uses the ratio of equivalents per million (epm) of SO_4 and Cl to those of alkalinity:

$$LSkI = \frac{(epm\ Cl^- + epm\ SO_4^{2-})}{(epm\ HCO_3^- + epm\ CO_3^{2-})}$$

The index was developed empirically from in situ measurements of corrosion in steel lines transporting Great Lakes water in the USA and may not have application in water with extremes of alkalinity. Index values of less than 0.8 indicate water with a tendency to form carbonate scales; 0.8 to 1.2 indicates scale formation may be inhibited, and over 1.2 indicates a tendency for corrosion.

Corrosion can cause major problems for borehole functionality, durability and groundwater quality. A groundwater with a strong tendency for scaling can also lead to problems with coatings on borehole infrastructure and pipes, which will greatly affect pumping efficiency. The state of groundwater with respect to carbonate equilibrium can therefore be considered most optimal for hand-pump longevity if neither show strong corrosion or scaling potential.

3.4 PREDICTING CORROSION BASED ON GROUNDWATER CHEMISTRY

We attempted to predict handpump components' corrosion based on groundwater chemistry, using L1-regularised logistic regressions over normalised chemical concentrations, corrosion and scaling indices, and control variables such as borehole age. This allowed us to derive explainable, probabilistic predictions, even when the number of predictors exceeded the number of observations. We assessed the regression models using predictive performance on held-out validation sets and the Bayesian information criterion (BIC).

To predict corrosion in handpumps, we first had to define when each pump component was corroded. We followed MacAllister et al. (2022) in considering each handpump to consist of rising mains, rods, and three grouped categories of components:

- above ground and external (AGE)
- above ground and internal (AGI)
- below ground (BG)

Table 2 lists, for each grouped category of component, the different handpump or component material types observed in the Hidden Crisis dataset and the subcomponents which constitute the grouped components and for which the dataset includes a condition description. Following MacAllister et al. (2022), we labelled a component as corroded if any subcomponent's condition description includes the words 'corroded', 'corrosion', 'encrusting', 'encrustation', or 'encrusted'. Whilst descriptions like 'encrustation' could in theory refer to scaling rather than corrosion, it was only corrosion that could be observed in the photographs of components with such descriptions.

Table 2 Subcomponent descriptions within the Hidden Crisis dataset.

Component	Component material /handpump types	Described subcomponents
AGE	Afridev; India Mark	Head; spout; handle; pump stand; top flange; water tank; bottom flange
AGI	Afridev; India Mark	Bearings; pump chain; hanger; fulcrum; pins
BG	Afridev; India Mark	Cylinder; plunger; seals; suction pipe; foot valve; reducers; check valve
Rising main	Al; galvanised iron; PVC	Section; thread; socket
Rod	Stainless steel; galvanised iron; PVC; fibreglass	Section

To examine the relationship between water chemistry and corrosion, we defined control variables that accounted for components' age and exposure to groundwater, and the physical properties of the corresponding borehole. We estimated the age A of each component as the number of years between its hand pump's installation and the year 2017, in which the component condition survey was conducted, and used the logarithm $\log A$ of component age and the measured groundwater temperature T as input variables in all analyses.

For each rod and each rising main, we also estimated exposure to groundwater by calculating the depth D_i of the component's midpoint: for a rod, the sum of half the rod's own length and the lengths of all rods above it, and the equivalent for rising mains. If D_i was greater than the maximum manually measured depth to groundwater in the borehole's pumping test, the

component was defined as ‘immersed’ in groundwater. If D_i was less than this maximum, but greater than the corresponding minimum manually measured depth to groundwater, the component was defined as ‘exposed’ to groundwater. For analyses of rod and rising main corrosion, we used the two binary indicators of immersion and exposure as additional input variables, alongside the minimum depth to groundwater, the difference between the minimum and maximum depths to groundwater, and the total borehole depth.

We wished to consider the relative importance of different input variables, so had to ensure input values were comparable during model fitting. To do so, we normalised input variables with respect to baseline values and excluded examples for which data was missing. We took these baseline values:

- pH: 7
- Eh: 300 mV
- RSI and PSI: 6
- LSI, LSkI and calcite saturation: 0
- all chemical concentrations: 0 mg/L

specific electrical conductance (SEC): 0 µS/cm

- $\log A$: 0
- temperature: 0°C
- borehole depth measurements: 0 m

Writing $\sum_k \cdot$ for a sum over all borehole indices k, we then defined normalised values X_{ij} for each borehole-level variable value x_{ij}, with i indexing the n_j boreholes for which a measurement of variable j exists, and variable baseline x_{0j}:

$$X_{ij} = \frac{x_{ij} - x_{0j}}{\sqrt{\frac{1}{n_j}\sum_k (x_{kj} - x_{0j})^2}}.$$

These normalised values, together with dummy values $X_{i0} = 1$, defined a dimensionless design matrix X for each type of each component, with each row representing a specific component of that type and with missing values where measurements were absent. For each type of rod and rising main, normalised values were repeated for each component of that type in the same borehole and we supplemented the design matrix with each component’s binary indicators of immersion and exposure. We then excluded from our analyses any component for which a subcomponent’s condition description is missing or includes the words ‘n/a’, ‘nan’, ‘non’, ‘not present, ‘missing’, ‘misses’, ‘dnk’ (‘do not know’) or ‘stolen’.

Since corrosion is probabilistic and there are many potentially relevant input variables, we predicted corrosion by fitting L1-regularised logistic regression models. Specifically, for each component i, we first defined the corrosion indicator y_i, equal to 1 if the component was corroded and 0 otherwise, and assumed that these indicators were independent. We then assumed a logistic model for predictions of corrosion probability P_i, with set I of input variables and corresponding variable coefficients β_j.

Specifically, for $\sum_{j\in I} \cdot$ a sum over all indices j in set I, we suppose:

$$P_i(\boldsymbol{\beta}) = \sigma\left(\sum\nolimits_{j\in I} X_{ij}\beta_j\right) = \frac{1}{1 - \exp\left(-\sum_{j\in I} X_{ij}\beta_j\right)}.$$

For each type of component, we defined the cross-entropy loss over the set C of components:

$$\mathcal{L}(C, \boldsymbol{\beta}) = -\sum\nolimits_{i\in C} [y_i \log P_i(\boldsymbol{\beta}) + (1 - y_i)\log(1 - P_i(\boldsymbol{\beta}))].$$

We used the Python package scikit-learn to seek the best-fit coefficients $\hat{\beta}_j$ that minimised the L1-loss for regularisation strength λ:

$$\mathcal{L}_\lambda(C, \boldsymbol{\beta}) = \mathcal{L}(C, \boldsymbol{\beta}) + \lambda \sum\nolimits_{j\in I} |\beta_j|$$

Where possible, we used five-fold cross-validation and the one-standard-error rule to determine the highest optimal regularisation strength. If fewer than five components were corroded, such cross-validation was impossible and we used the regularisation strength $\lambda = 1$. Otherwise, we randomly split the set of components into five subsets C_k, with approximately equal sizes $|C_k|$ and at least one corroded component in each. Then, for each regularisation strength λ_l in the range $2^{-10}, 2^{-9.5}, \ldots, 2^{10}$, we held out each subset in turn, identified the coefficients $\hat{\beta}_{j,k}(\lambda_l)$ that minimised L1-loss over the other four subsets $\mathcal{L}_{\lambda_l}(C \setminus C_k, \boldsymbol{\beta})$, calculated the corresponding cross-entropy loss over the held-out subset $\mathcal{L}(C_k, \widehat{\boldsymbol{\beta}}_k(\lambda_l))$, and calculated the average and standard error of the per-component loss:

$$\bar{\mathcal{L}}(\lambda_l) = \frac{1}{5}\sum_k \frac{1}{|C_k|}\mathcal{L}\left(C_k, \widehat{\boldsymbol{\beta}}_k(\lambda_l)\right), \qquad \delta\mathcal{L}(\lambda_l) = \sqrt{\frac{1}{20}\sum_k \left(\frac{1}{|C_k|}\mathcal{L}\left(C_k, \widehat{\boldsymbol{\beta}}_k(\lambda_l)\right) - \bar{\mathcal{L}}(\lambda_l)\right)^2}.$$

Given these values, we followed Hastie et al. (2009) in selecting the highest regularisation strength that was within the standard error of the loss-minimising regularisation strength $\lambda_{min} = \mathrm{argmin}_{\lambda_l}\bar{\mathcal{L}}(\lambda_l)$:

$$\lambda = \max(\{\lambda_l : \bar{\mathcal{L}}(\lambda_l) < \bar{\mathcal{L}}(\lambda_{min}) + \delta\mathcal{L}(\lambda_{min})\}).$$

To assess each of our cross-validated logistic regression models, we compared the values of the cross-validation likelihood and of the BIC to those of a baseline model, in which the probability of corrosion was constant over examples of a given component type. We used $\mathcal{L}(C, I)$ for the cross-entropy loss over component set C for input variable set I, after the optimisations of $\beta_{j,k}$, λ_l, and β_j, and write $\bar{\mathcal{L}}(C, I)$ for the corresponding average per-component loss during cross-validation.

To assume a constant probability of corrosion is equivalent to using only dummy variables as input, $I = \{0\}$., so the difference in BIC between our inputs-I model and the baseline model is:

$$\Delta BIC = (|I| - 1)\ln(|C|) + 2\mathcal{L}(C, I) - 2\mathcal{L}(C, \{0\}).$$

A value less than zero indicates that the inputs-I model provides more information about corrosion than the baseline model, with lower values indicating more informative models.

In contrast, a more informative model is indicated by a greater relative cross-validation likelihood:

$$\Lambda = \exp[\bar{\mathcal{L}}(C, \{0\}) - \bar{\mathcal{L}}(C, I)].$$

Λ is equal to one when cross-validation observations are equally likely under the inputs-I model and the baseline model.

For each component type, we first attempted to construct the most informative model for corrosion, by considering the largest possible reasonable set of input variables. No Al rising mains or fibreglass rods exhibited corrosion, so no analysis was possible for these component types. For each other component type, we conducted the analysis with an input set I of all variables in Appendix 2 (Table A2), except those for which more than 10 % of the relevant components lacked a measurement, and with a component set C of all relevant components, except those for which a measurement in set I was missing. For the BG component of Afridev pumps and the AGI component of India Mark handpumps, fewer than five components exhibited corrosion, so no cross-validation was possible.

In many settings, fewer water chemistry data are available than in this study, so it will be difficult or impossible to apply the described ‘all inputs’ models. For broader applicability, we repeated analyses with simpler input variable sets that are more likely to be available: individual, binary indicators, based on pH and corrosion indices. Specifically, we took I to be, in turn, the combination of the dummy variable 0 and binary indicators of each of the conditions in Appendix

2 (Table A3), including for rods and rising mains the binary control variables indicating exposure and immersion.

3.5 PREDICTING GROUNDWATER CHEMISTRY BASED ON CORROSION

The data available to us were observational, so to examine the effect of corrosion on water chemistry we had to exclude the effect of water chemistry on corrosion. To do so, we estimated the difference in chemistry between the water in an aquifer, presumed unaffected by pump components and their corrosion, and the water in the pump's borehole, which can be strongly affected by such corrosion. We derived this estimate by subtracting the measurements taken in Survey 2, after a pumping test and the borehole's replenishment from the aquifer, from those taken in Survey 1, in water with prolonged exposure to the pump components. The full set of variables for which such an estimate y_i could be calculated is listed in Table A1.

For each water chemistry variable for a given borehole, we considered as potential influences both the number of components of each type and the number of corroded components of each type. A component may leach solutes without exhibiting corrosion and corrosion may be associated with specific solutes; both sets of solute may influence water chemistry. We did not regard as accurate any labelling of PVC components as 'corroded', so did not include these counts. We used x_{ij} for the number of components of type j in borehole i, with corroded components distinguished, and calculated normalised input variable value X_{ij} as in Section 3.4.

Since we have many potential groundwater chemistry influences on corrosion, we again conducted L1-regularised regression models, but we then used a linear link function. Water-chemistry variable values y_i are continuous, so we took predicted values $\hat{y}_i$ to be linear functions of input variables:

$$\hat{y}_i(\boldsymbol{\beta}) = \sum_{j \in I} X_{ij} \beta_j,$$

And defined a corresponding squared error loss:

$$\mathcal{L}(C, \boldsymbol{\beta}) = \sum_{i \in C} [y_i - \hat{y}_i(\boldsymbol{\beta})]^2.$$

Except for these changes of definition, we conducted the same model-fitting process as in Section 3.4.

Because Survey 1 and Survey 2 were conducted at different times, with many measurements taken according to slightly different methodologies, there is wide scope for confounding factors. We therefore conducted a second analysis of hand-pump influences on water chemistry, attempting to predict the water chemistry measured in the borehole, in Survey 1, using the numbers of components of each type. Under the assumption that the component types within a borehole are independent of the corresponding aquifer's water chemistry, successful predictions correspond to changes in water chemistry due to pump components.

4 Results

4.1 GROUNDWATER CHEMISTRY

The groundwater-chemistry data show a very large range of compositions, both within and between the three countries. Major cations and anions are mixed, but Ethiopian groundwater is largely Ca-Na-HCO_3 water, Malawi Na-Ca-HCO_3-SO_4-Cl water and Uganda Na-HCO_3-SO_4-Cl water. The Malawi dataset has a larger proportion of TDS greater than 1000 mg/L samples, which corresponds with the higher Na, Cl and SO_4 concentrations (Figure 7).

Groundwater temperature spans a lower range in Ethiopia than the other countries, as the study area is in the Ethiopian Highlands and hence has higher elevation. Temperature ranges are (both surveys):

- Ethiopia: 16.8 to 28.4°C
- Malawi: 22.4 to 36.2°C
- Uganda: 21.1 to 32.2°C

Groundwater pH ranges from 4.7 to 8.8, with most samples around 6 to 7 (Figure 8). Ethiopian groundwater has the highest median and maximum pH values in the dataset. This groundwater derives from Cenozoic volcanic rocks (mafic or silicic). The Ugandan groundwater samples have the lowest median pH values. These derive from Precambrian granulite, gneiss or metasediment. All three countries have a minority of groundwater samples with pH values less than 6: 1.8, 9.6 and 10.6 % across both surveys for Ethiopia, Malawi and Uganda, respectively.

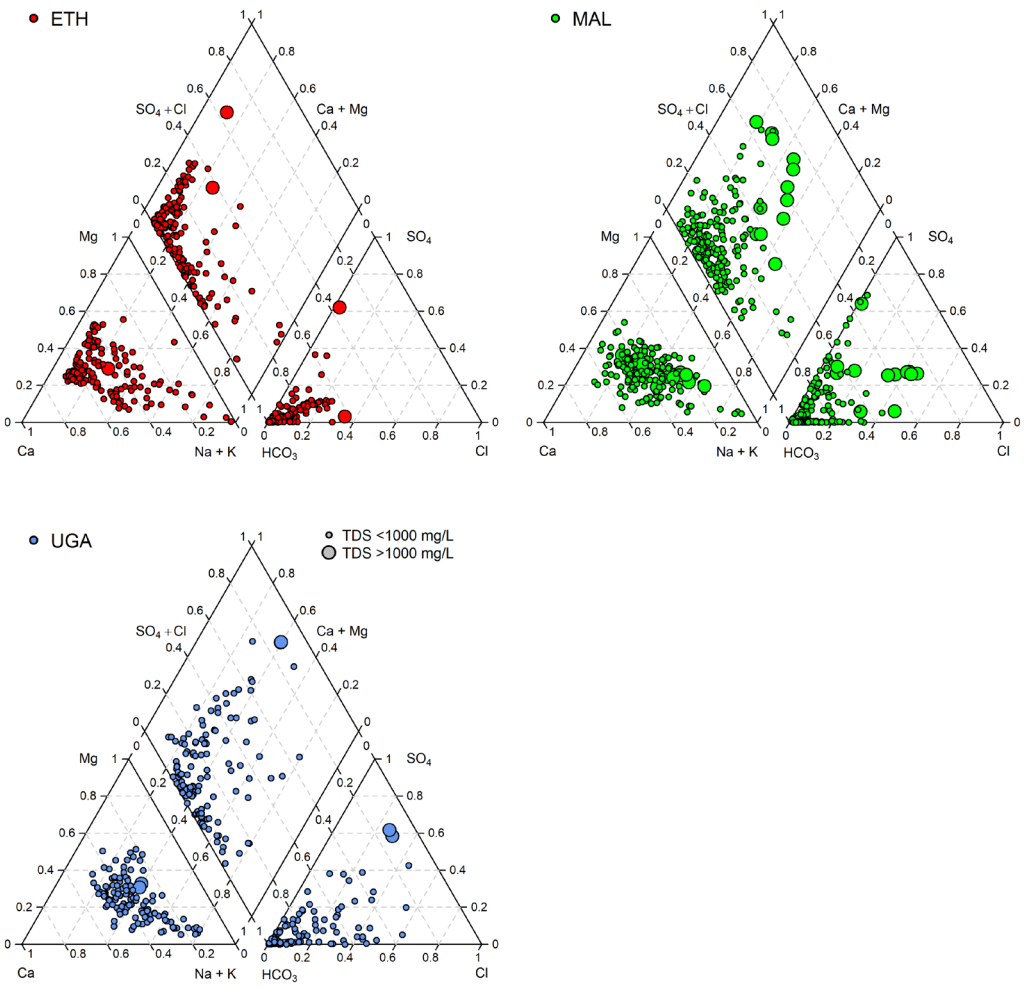

Figure 7 Piper diagrams for the groundwater samples from Ethiopia (ETH), Malawi (MAL) and Uganda (UGA), distinguished also by TDS (both surveys). BGS © UKRI 2026.

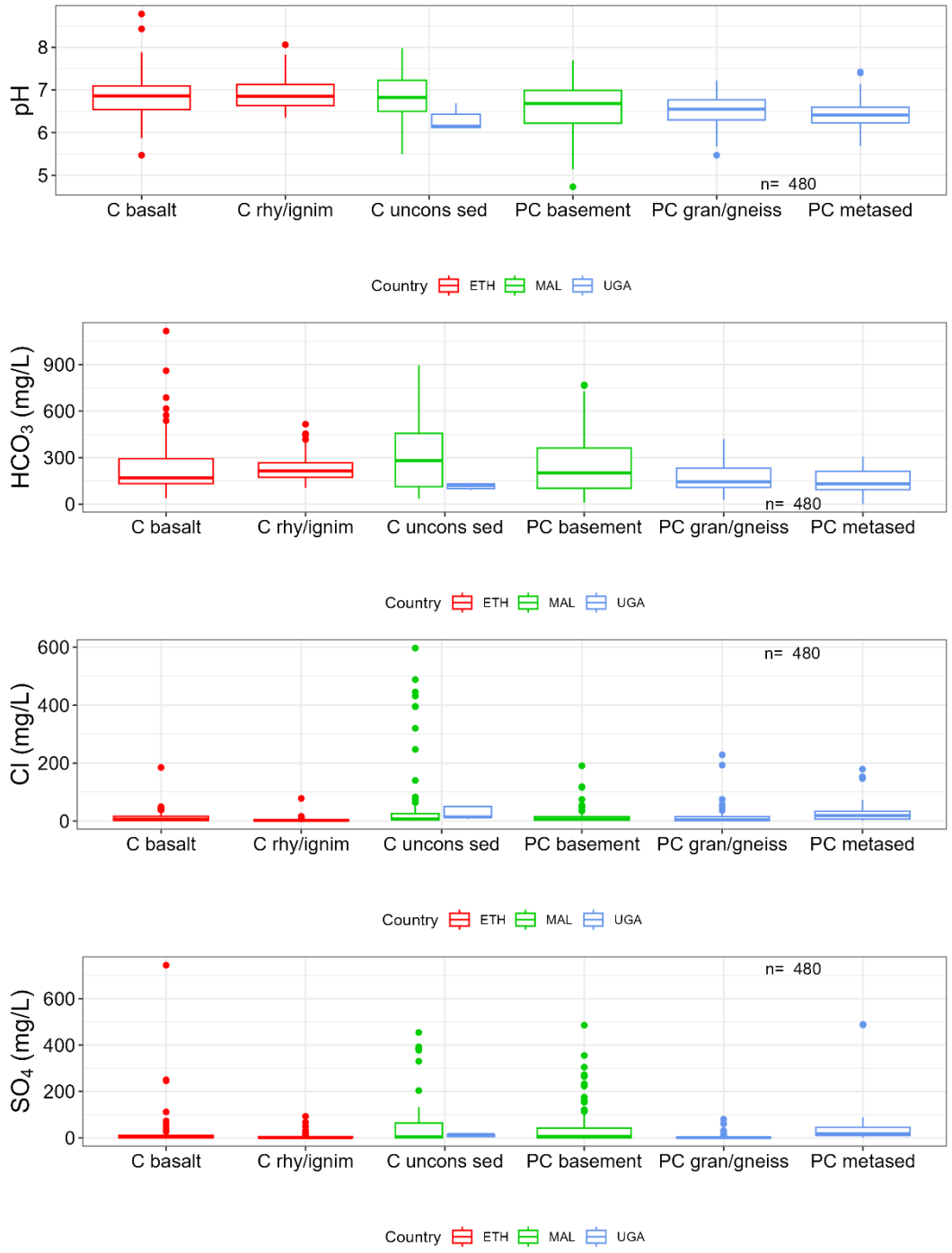

Figure 8 Box plots of pH, HCO_3, Cl and SO_4 in groundwater samples from both surveys, distinguished by country and geology. C: Cenozoic; PC: Precambrian; rhy: rhyolite; ignim: ignimbrite; uncons: unconsolidated; gran: granulite, metased; metasediment. Shows samples with charge balances better than ±10%. BGS © UKRI 2026.

Alkalinity (HCO_3) has a clear association with pH, notably for the Malawi and Uganda samples (correlation coefficient 0.66 for Malawi and 0.63 for Uganda, lower at 0.28 for Ethiopia; 0.53 for all combined; p values all <<0.05). Alkalinities are highest (up to 1120 mg/L) in the Ethiopian samples and lowest in the crystalline rocks of Uganda (Figure 8). Figure 8 also shows the large range of Cl and SO_4 concentrations represented in the groundwaters and the more common high values found in the Malawian samples.

Figure 9 shows the ranges of DO and manganese (Mn) in the groundwater samples. Compositions are commonly oxic, with DO typically greater than 0.3 mg/L and an observed median of 1 mg/L. Oxic conditions are consistent with observations of the groundwater having young components and flowing via rapid transit pathways, evidenced by the presence of

Escherichia coli and young chlorofluorocarbon/sulphur hexafluoride ages from many sites (Banks et al., 2021). Nonetheless, ranges extend to low concentrations and so some sub- or anoxic conditions are represented, suggesting more limited flow. Concentrations of Mn are mostly less than 40 µg/L but with some 12 % occurring as outliers, reaching up to a maximum of 1 mg/L.

Variations of Mn with pH and Eh (Figure 10) indicate that the highest concentrations tend to be in samples with pH in the approximate range of 6.3 to 7.3 and Eh less than 300 mV. The lowest pH values occur in low SEC samples (less than 200 µS/cm) where concentrations of most solutes including Mn are low. Mn appears to have a stronger relationship with Eh, being soluble in mildly reducing conditions. The highest Mn concentrations are found in groundwater samples from Malawi and Uganda (Figure 10).

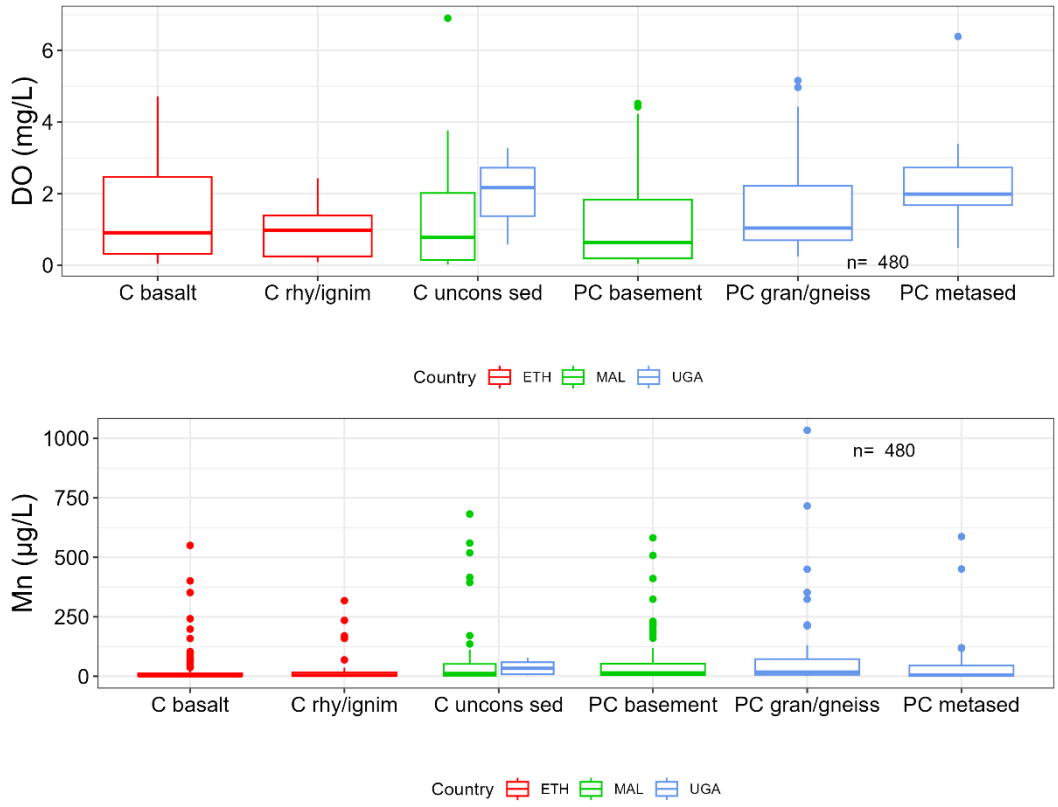

Figure 9 Box plots of DO and Mn in groundwater samples from both surveys, distinguished by country and geology. Abbreviations as for Figure 8. Shows samples with charge balances better than ±10 %. BGS © UKRI 2026.

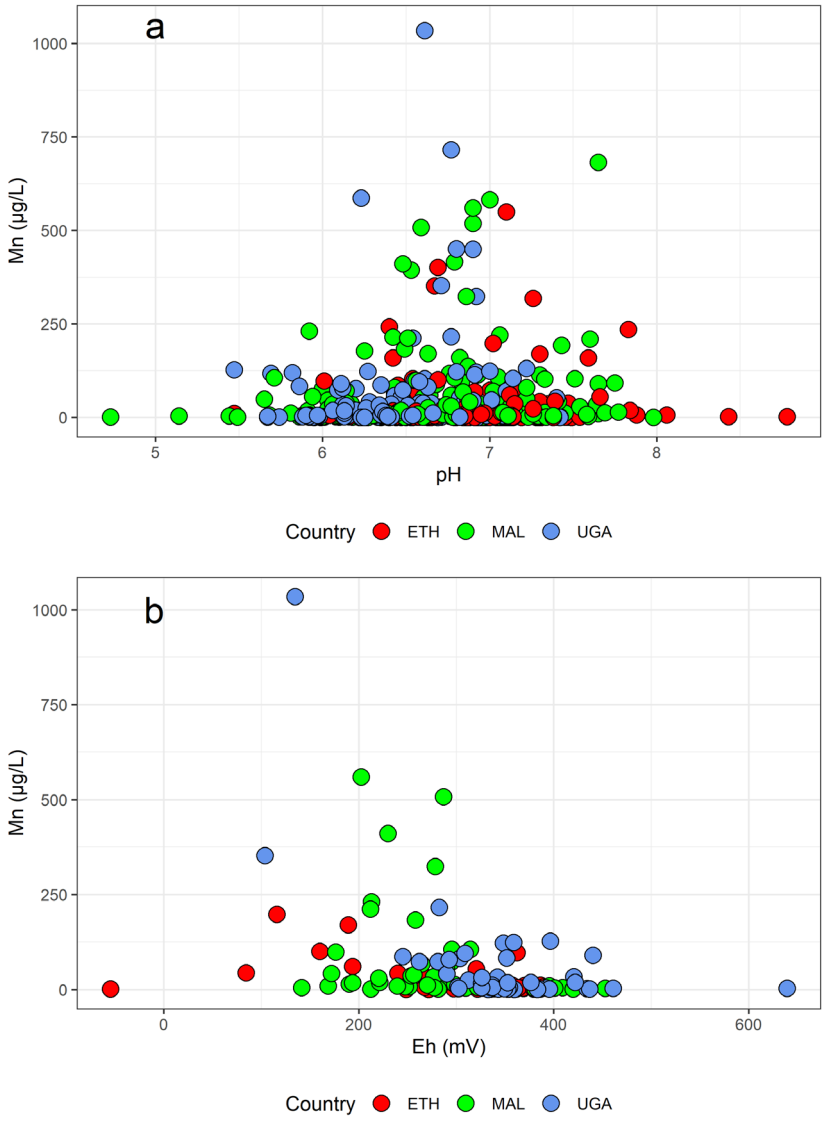

Figure 10 Variation of Mn with a) pH and b) Eh in the groundwater samples, distinguished by country. BGS © UKRI 2026.

Eh/pH diagrams for Fe and Mn (Figure 11) show the distribution of groundwater samples from Ethiopia, Malawi, and Uganda, respectively. Groundwater in each country spans the range between oxic and sub- or anoxic conditions. For Fe, this means samples straddle the fields of mineral $Fe(OH)_3$ and dissolved Fe^{2+}dominance, with around half of samples in each category (more oxic conditions with a higher proportion as $Fe(OH)_3$ in Ethiopian samples).

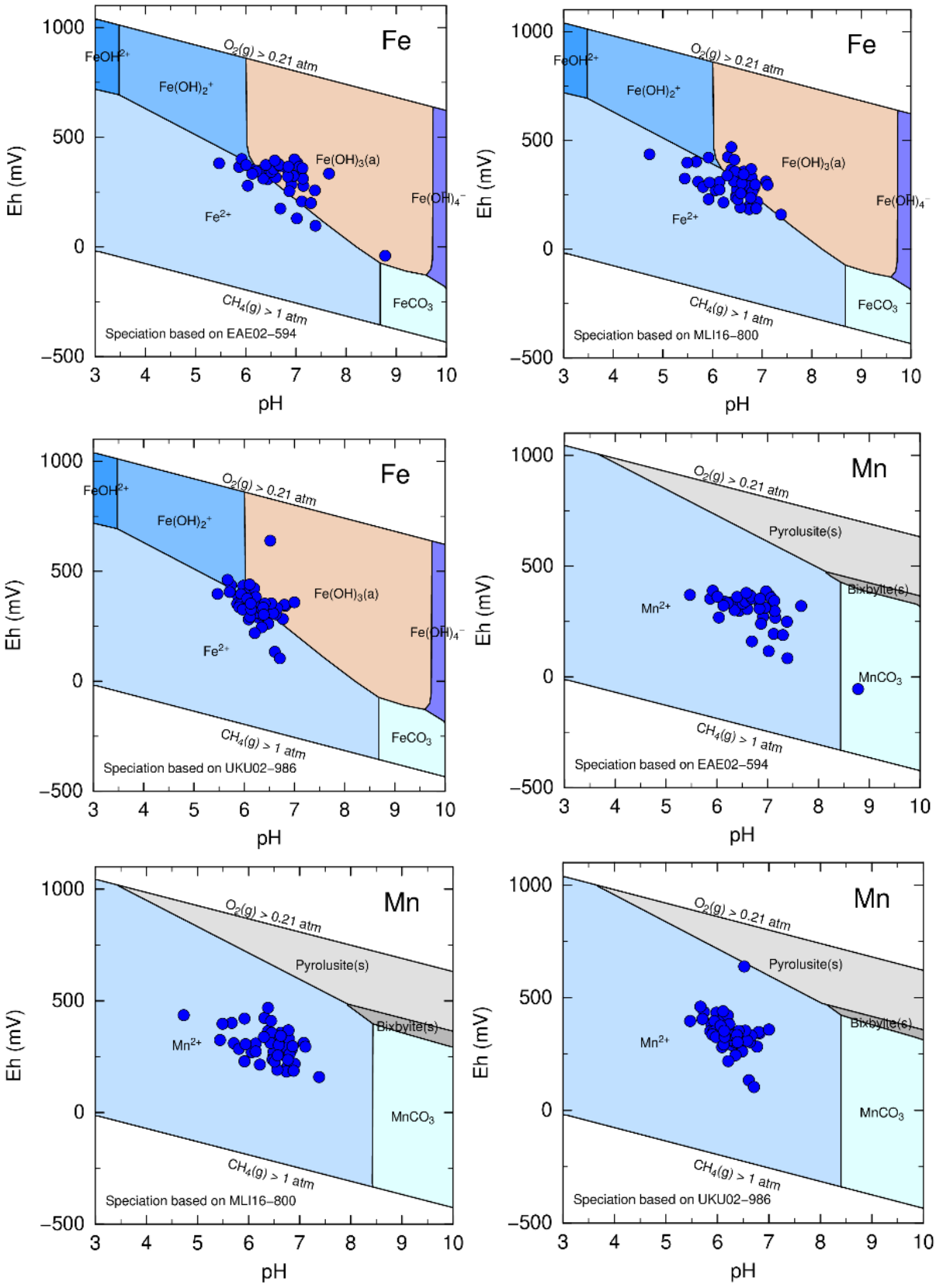

Figure 11 Predominance of species of (top) Fe in Ethiopia, Malawi and Uganda, respectively, and (bottom) Mn in Ethiopia, Malawi and Uganda, respectively; also showing pH and Eh values for groundwater samples from the three countries. Speciation is based on compositions of individual samples from each country, using PHREEQC, PhreePlot and the `wateq4f.dat` database (Kinniburgh and Cooper, 2004). Solutes are in shades of blue, solids in brown or grey.

For Mn, dissolved Mn^{2+} is likely the dominant species for all samples, while for Fe, dissolved Fe^{2+} is dominant for around half of the samples (fewer for Ethiopian samples; Figure 11). The plots are dependent on the quality of field data for pH and Eh but suggest that many samples of groundwater are sufficiently reducing to support dissolved Fe and Mn and that distributions may be due at least in part to the aquifer conditions rather than necessarily indicating metal corrosion as the dominant control on dissolved concentrations.

Box plots of the distributions of trace metals that could potentially be derived from borehole metalwork are shown by sampling survey in Figure 12. As noted in Section 3.1, samples from Survey 1 were collected after 30 minutes of pumping while those from Survey 2 were collected after 2.5 hours of pumping tests. Therefore, it might reasonably be inferred therefore that Survey 2 samples are more representative of aquifer conditions.

Figure 12 shows paired samples (sampled from the same sites in surveys 1 and 2). Higher median values are seen in the Survey 1 dataset for Cr and Cu, with a slightly higher median value for Pb. Ranges for Fe need to be treated with caution because the results from Survey 1 were analysed by ICP-OES and so have a higher detection limit (100 µg/L). They are included here to compare the upper ends of the ranges: these are higher for Survey 2. Difference between medians is indistinct for Mn and median values are higher in Survey 2 datasets for Ni and Zn.

A Wilcoxon signed-rank test for median differences between two datasets containing censored data (using `cen_signedranktest` from the NADA2 package in R) suggests that median differences were significantly higher (p less than 0.05) in Survey 1 only for Cr and Cu. It is therefore tentatively concluded that Cr and Cu may have a contribution from the borehole infrastructure while the other trace metals investigated are likely dominantly derived from the aquifer.

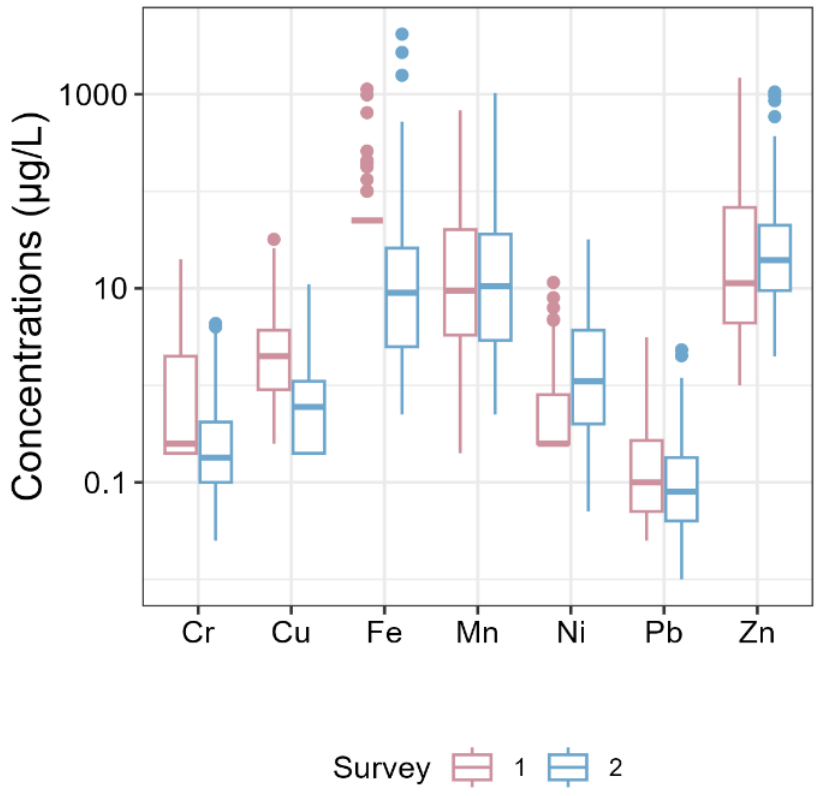

Figure 12 Box plot of the distributions of selected trace metals, organised by sampling survey (charge balances better than ±10 %). Non-detects are plotted as 0.5 × detection limit. Data for Fe in Survey 1 was measured by ICP-OES and has high detection limits (100 µg/L), which has truncated the lower end of the distribution. Note also that the lower bar for Fe concentrations equates to both the minimum and median observation as most Fe analyses by ICP-OES were non-detects.

Box plots of the concentrations of Cr, Ni, Pb and Zn in Survey 2 samples, organised by country and geology, are shown in Figure 13. These are taken to be potentially less impacted by borehole metalwork contamination because of the longer (2.5 hour)s borehole purge. The plots show a number of outliers, but the distributions of the highest concentrations are largely sporadic. Precambrian granulite and metasediments in Uganda appear to have the highest maximum concentrations of the four metals.

Of the trace metals with associated World Health Organization (WHO) drinking-water guideline values, most do not show exceedances. Exceptions are Mn, for which 15 % exceeded the WHO provisional guideline value of 80 µg/L, and uranium (U), for which one sample (0.7 %) exceeded the WHO provisional guideline value of 30 µg/L. Of the non-metals, 3.1 % exceeded the guideline value for fluoride (F) and 2.9 % for nitrate (NO_3) (both surveys included).

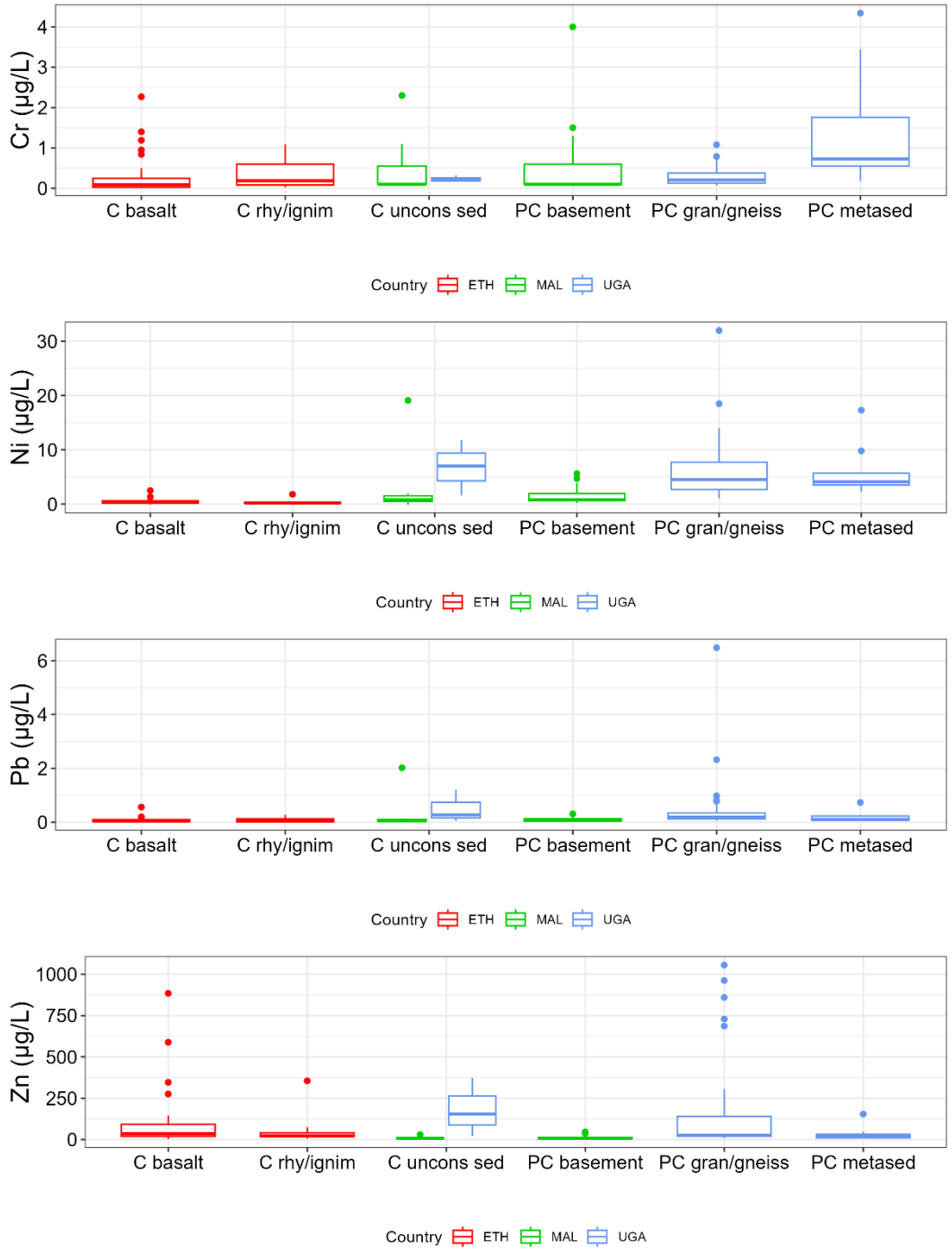

Figure 13 Box plots of Cr, Ni, Pb and Zn in groundwater samples from Survey 2, distinguished by country and geology. Abbreviations as for Figure 8. Shows samples with charge balances better than ±10 %. BGS © UKRI 2026.

Of the trace metals with associated WHO drinking water guideline values, most do not show exceedances. Exceptions are Mn, for which 15% exceed the WHO provisional guideline value of 80 µg/L and U for which 1 sample (0.7%) exceeded the WHO provisional guideline value of 30 µg/L. Of the non-metals, 3.1% exceeded the guideline value for F and 2.9% for NO_3 (both surveys included).

4.2 SATURATION AND CORROSION INDICES

Box plots of the ranges of values for the $SI_{calcite}$ and LSI, RSI, PSI and LSkI indices are shown in Figure 14. Both $SI_{calcite}$ and LSI indicate that most groundwaters (85 %) in the database are undersaturated with respect to calcite, many significantly so. More samples from the Cenozoic unconsolidated sediments in Malawi are saturated or oversaturated than any other sample group. The majority of samples in the database also exceed 8 on RSI (74 %) and 6.5 on PSI (78 %), both indicating a tendency towards corrosion. By contrast, the majority of analyses (96 %) have an LSkI less than 1.2, which would suggest non-corrosive or even scaling conditions. This discrepancy might be because of the extremes of alkalinity represented in the groundwater samples, which are beyond the range of application of the index (Section 3.3).

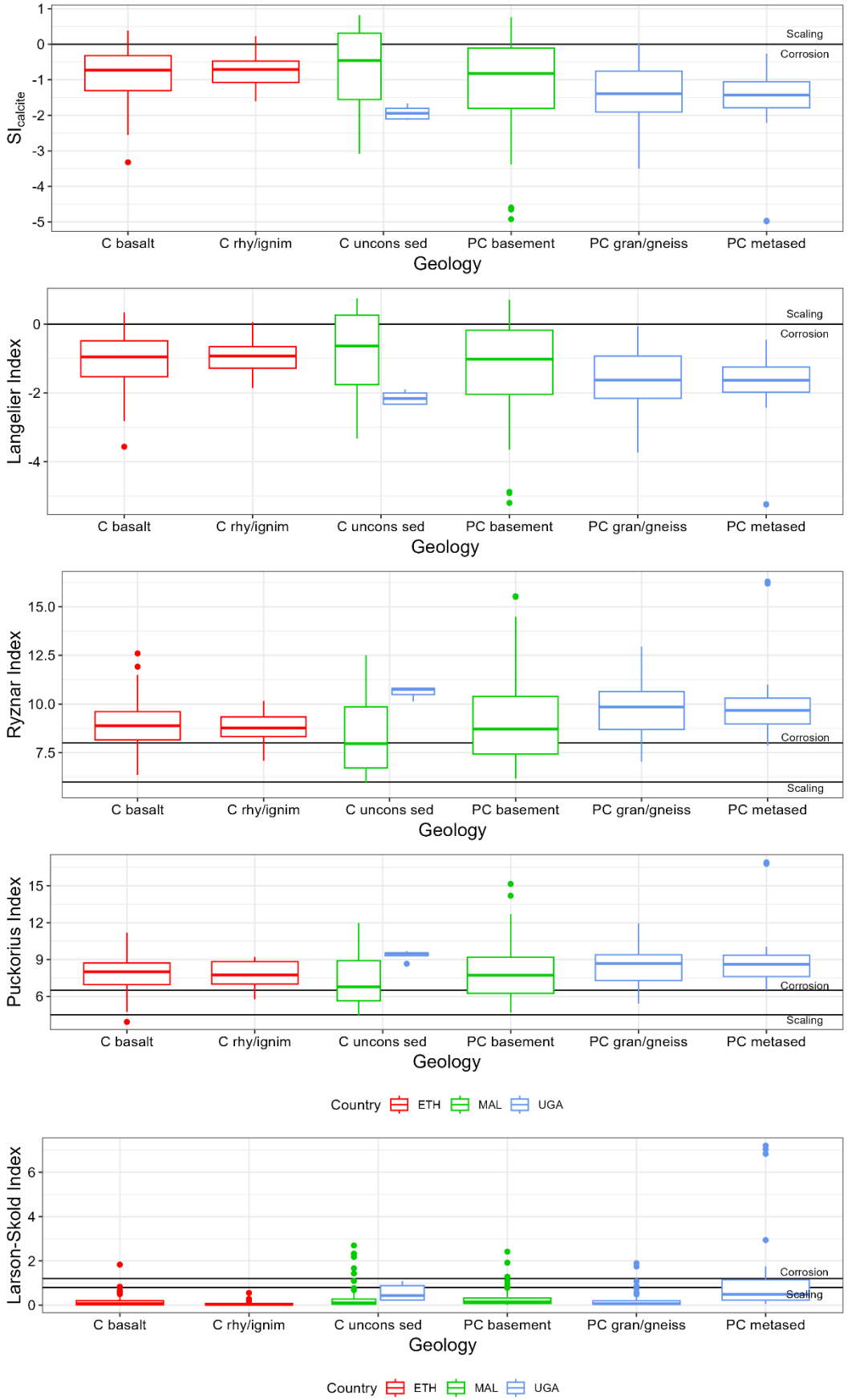

Figure 14 Calcite saturation and corrosion indices, organised by country and geology, showing the approximate thresholds for conditions likely to result in scaling or corrosion. BGS © UKRI 2026.

4.3 PREDICTING CORROSION BASED ON WATER CHEMISTRY

The best-performing corrosion prediction models are summarised in Table 2, which forms the basis for this section.

We first consider those models that predict the corrosion of the AGE, AGI and BG components of hand pumps, examining the baseline-relative difference ΔBIC in the BIC, as defined in Section 3.4. Of the models for these at-surface components' corrosion, the only one more informative than the baseline, with $\Delta BIC = -0.655$, was that using the 'pH less than 7.0' indicator to predict the corrosion of Afridev pumps' BG component. However, the sample of such components includes few examples of corrosion, the improvement in BIC is very small and lower pH is associated in the model with a lower corrosion probability, so this effect is likely to have arisen by random chance. In general, the numbers of corroded at-surface subcomponents are low, so that disparate subcomponents must be aggregated for analysis, and our statistical models do not effectively predict corrosion of these aggregated AGE, AGI and BG components.

Table 3 Performance of the model for each component type using all available inputs and of the two best-performing models using a binary indicator as input. |C| indicates the number of components in the sample; $\sum_i y_i$ the number of corroded components, and λ the regularisation strength. Performance better than a dummy-input-only model is indicated by relative likelihood Λ greater than 1 and BIC difference ΔBIC less than 0.

Handpump Type	Component	Inputs	$\|C\|$	$\sum_i y_i$	λ	Λ	ΔBIC
Afridev	AGE	All inputs	65	15	5.7	0.991	4.59
		Calcite<0	72	18	4.0	0.979	1.09
		pH<7.0	72	18	4.0	0.988	1.09
	AGI	All inputs	59	10	4.0	0.973	17.41
		Calcite<0	65	11	4.0	0.981	1.49
		pH<5.5	65	11	2.8	0.989	0.78
	BG	All inputs	64	2	1.0	N/A	21.56
		pH<6.5	70	3	1.0	N/A	0.29
		pH<7.0	70	3	1.0	N/A	-0.65
India Mark	AGE	All inputs	69	14	11.3	0.895	12.54
		Calcite<0	71	14	4.0	0.986	1.26
		pH<6.5	71	14	4.0	0.986	1.26
	AGI	All inputs	65	2	1.0	N/A	47.07
		Calcite<0	67	3	1.0	N/A	0.29
		pH<6.5	67	3	1.0	N/A	0.29
	BG	All inputs	63	16	8.0	0.965	4.06
		Puckorius>7	65	16	2.8	0.991	0.62
		pH<5.5	65	16	4.0	0.985	1.20
Galvanised iron	Rising main	All inputs	549	205	8.0	1.220	-135.12
		Calcite<0	591	232	5.7	1.044	-43.24
		pH<6.5	591	232	11.3	1.074	-84.57
	Rod	All inputs	805	419	1.0	1.337	-347.65
		Larson-Skold>0.2	868	468	16.0	1.008	-16.72
		pH<6.5	868	468	16.0	1.014	-26.91
Stainless steel	Rod	All inputs	479	28	5.7	1.071	-3.99
		pH<6.5	534	40	11.3	1.016	-15.13
		pH<7.0	534	40	16.0	1.078	-85.13

For galvanised iron rising mains, meanwhile, we observe a strong effect of water chemistry on the probability of corrosion.

The most effective model is that to which all inputs are available, with a per-component observation likelihood ratio of $\Lambda = 1.22$ during cross-validation and with substantial difference in the BIC: $\Delta BIC = -131$. This is therefore the most appropriate model for purely predictive purposes, if applied in a similar context and setting to the present study and with equally detailed water chemistry datasets.

However, as Figure 15 shows, this model requires many different influences on corrosion to be considered, with 21 distinct variables determining predictions. It is unclear, for example, whether higher corrosion rates at higher total inorganic carbon (TIC) concentrations are due to carbonic acid reactions or because TIC is correlated with a different cause of corrosion. In contrast, the most effective single-binary-indicator model is less effective ($\Lambda = 1.07$; $\Delta BIC = -85$), but simple to apply and easy to interpret (the corrosion probability is 0.614 if pH is less than 6.5 and 0.306 if not, as in Figure 16

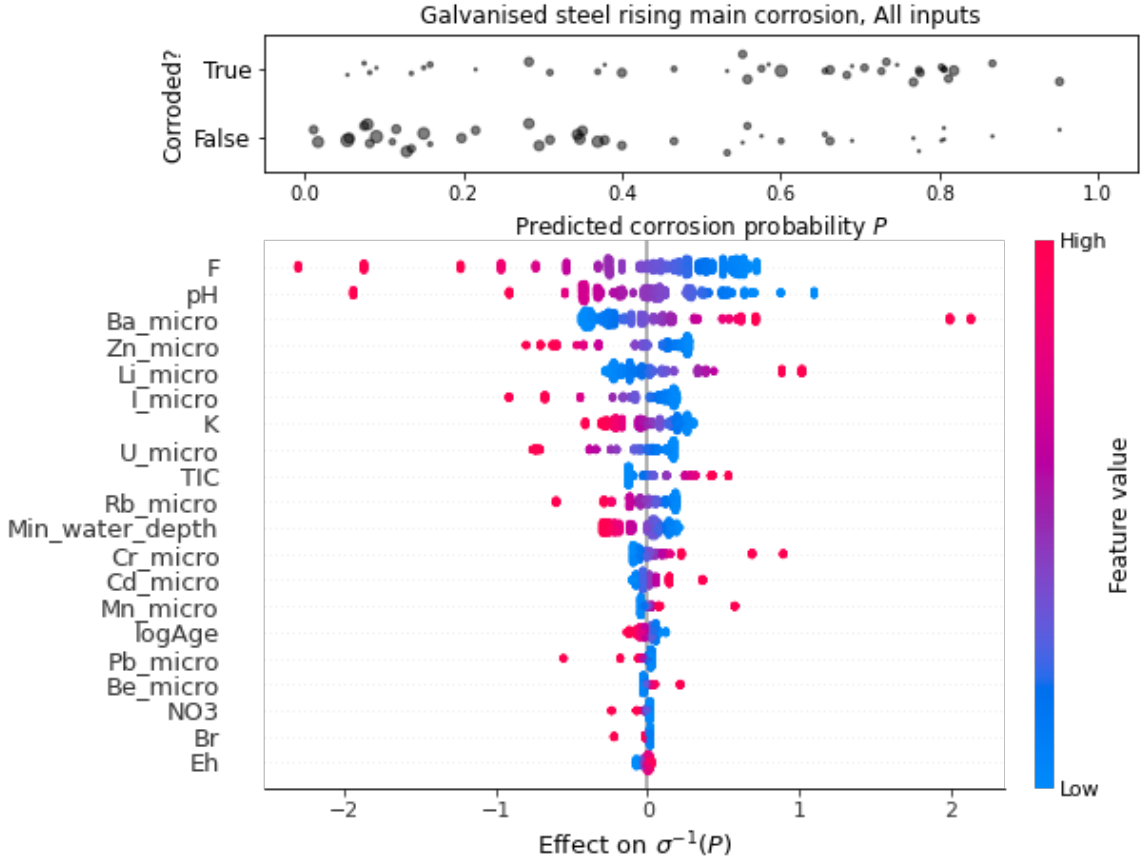

Figure 15 Predictions of the all-inputs model for the corrosion of galvanised iron rising mains. Top: predicted corrosion probabilities for components that do and do not exhibit corrosion. Y-axis scatter is introduced for visual clarity, while the size of dots corresponds to the number of observations. Components that exhibit corrosion tend to have higher predicted corrosion probabilities. Bottom: effects on predicted corrosion probabilities of the 20 most significant input variables. Each point in a row corresponds to an observation, with the colour indicating the normalised, unitless value of that row's input variable. Low pH values are associated with greater corrosion risk, but many input variables' effects are hard to interpret physically.

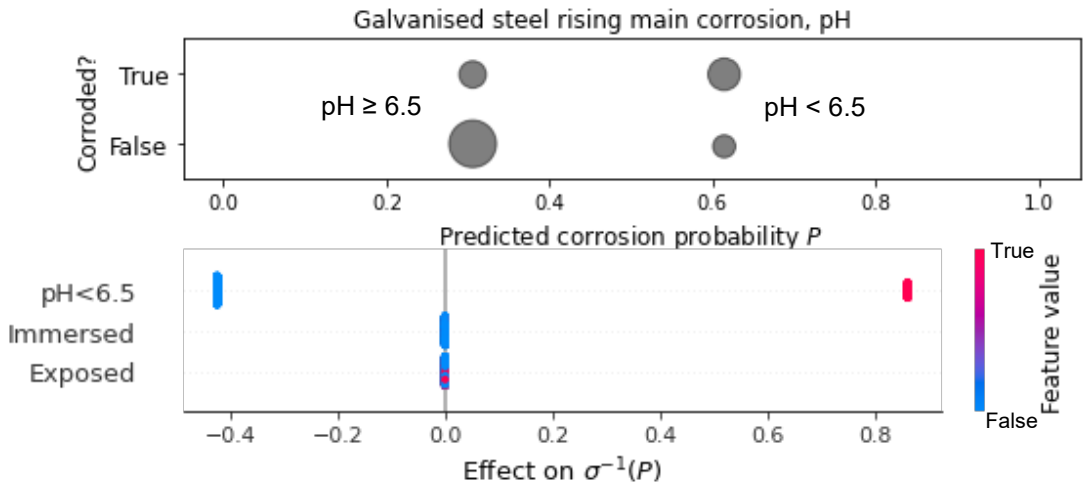

Figure 16 Predictions of the pH less than 6.5 model for the corrosion of galvanised iron rising mains. Details as for Figure 8. BGS © UKRI 2026.

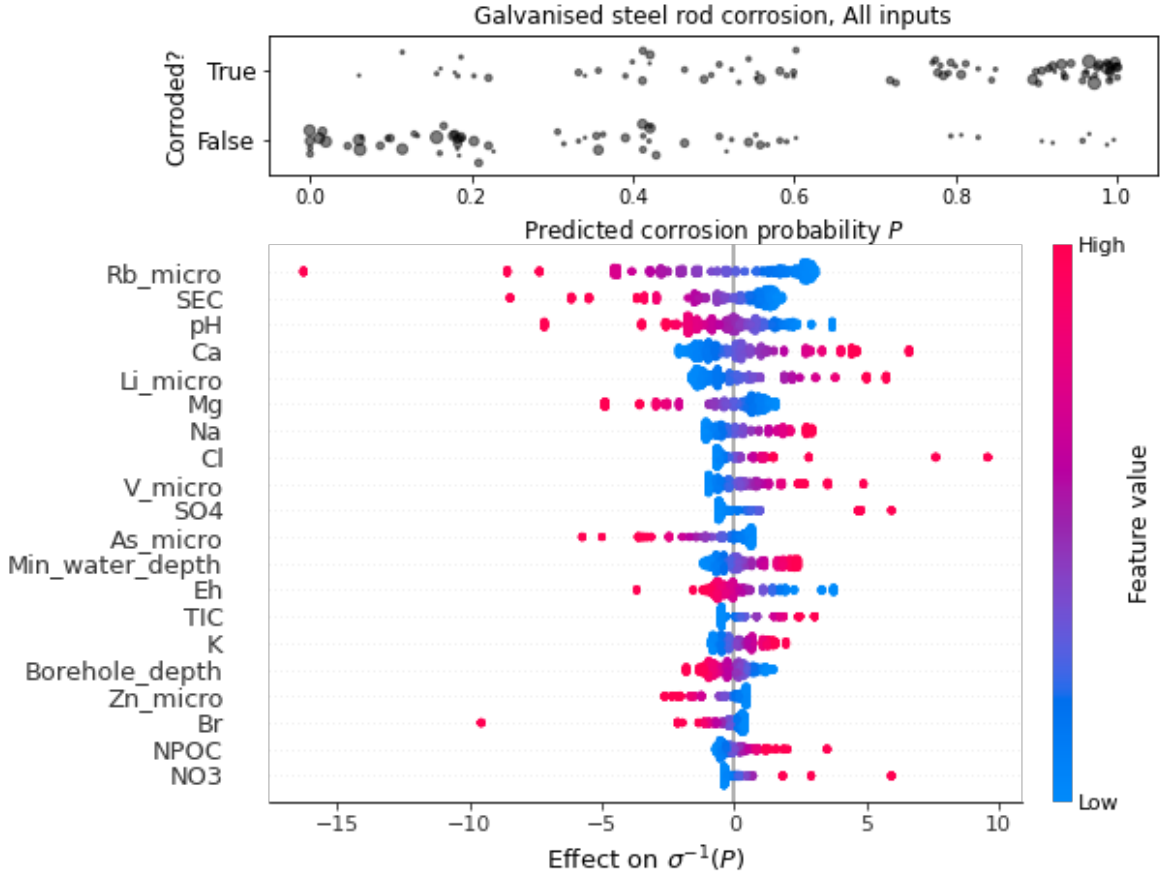

Figure 17 Predictions of the all-inputs model for the corrosion of galvanised iron rising mains. Details as for Figure 15. BGS © UKRI 2026.

Equivalent observations can be made about the corrosion of galvanised iron rods. The most effective single-binary-indicator model is simpler ($\Lambda = 1.014$; $\Delta BIC = -26.9$; corrosion probability is 0.613 if pH is less than 6.5; 0.500 otherwise), but by far the most effective model is that for which all inputs were available and 39 have an effect ($\Lambda = 1.34$; $\Delta BIC = -348$; probabilities in Figure 17). Thus, while the full-chemistry model maximises predictive accuracy, the simpler

pH-based model is more easily interpretable and perhaps better suited to practical decision making, particularly in data-limited or operational settings.

For stainless steel rods, our models suggest pH less than 7 was a more informative predictor of corrosion ($\Lambda = 1.078$; $\Delta BIC = -85.1$) than pH less than 6.5 ($\Lambda = 1.016$; $\Delta BIC = -15.1$). This model performed better than that to which all inputs were available ($\Lambda = 1.071$; $\Delta BIC = -4.0$, with 13 inputs having an effect). Furthermore, according to the model, the probability of corrosion is 0.064 when pH is less than 7 and 0.500 otherwise (Figure 18). However, corrosion was both uncommon and generally mild, which may the limit the models ability to identify robust predictors of stainless steel corrosion and may contribute to uncertainty in the model results. In our dataset, corrosion was only observed on 40 of 534 rods, of which 24 were from just two boreholes, and the results may be influenced by a number of confounding factors, including variations in groundwater chemistry, manufacture, installation, maintenance, or inconsistencies in corrosion recording. The observed relationship may reflect confounding factors or interactions between predictors, whereby pH acts as a proxy for other environmental or operational variables affecting corrosion. Alternatively, the pH threshold identified by the decision tree may represent a threshold artefact arising from the specific distribution of observations within the dataset.

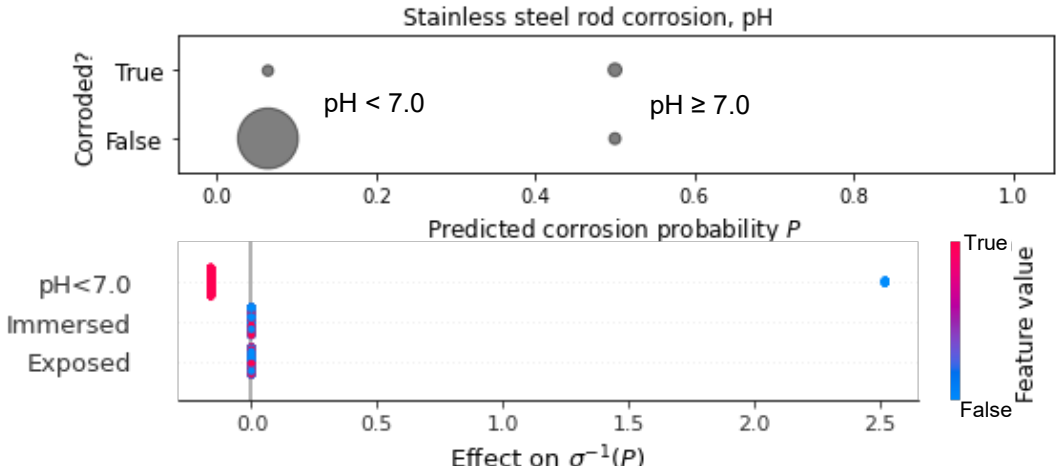

Figure 18 Predictions of the pH less than 7 model for the corrosion of stainless steel rods. Details as for Figure 15. BGS © UKRI 2026.

4.4 PREDICTING WATER CHEMISTRY BASED ON CORROSION

In our first analysis, we attempted to predict differences in water chemistry between a borehole and its aquifer based on counts of different component types and of corroded components of different type. In all best-fit models but one, none of these counts had any effect. The one exception was for differences in dissolved Al concentration, for which there were fewer than five measurements, and the results were not reliable.

In our second analysis, we attempted to predict the water chemistry in a borehole based on the types of components within that borehole. There was evidence of confounding factors within the dataset, for example with stainless steel rods and galvanised iron rising mains rarer at greater latitudes, but there was no evidence of any consistent effect of component type on water chemistry.

5 Discussion and conclusions

Investigations of the impacts of groundwater chemistry on corrosion and vice versa reveal key findings, these are discussed in the following sections.

5.1 OBSERVED PH

- pH values of less than 7 were common (73 % less than 7; 33 % less than 6.5)
- Despite its simplicity as an indicator of corrosion, interpretation of pH is reliant on good-quality data, requiring well maintained and regularly calibrated sensors

5.2 CORROSION INDICES

- Corrosion indices are proxies rather than direct indicators of metal corrosion; nonetheless, they are useful and widely used
- The water chemistry shows a large range of compositions from low-TDS to more than 1000 mg/L TDS, but an overwhelming majority of the corrosion indices indicate conditions that are potentially mildly or strongly corrosive and relatively few are scale-forming
- Corrosion indices can be calculated from a major-ion analysis and can provide prior warning of corrosion risk to inform borehole construction; again, these need to be based on good-quality data
- Both the calcite saturation index and the LSI indicate that most groundwaters in the database are undersaturated with respect to calcite, many significantly so
- The majority of samples in the database also exceed 8 on the RSI and 6.5 on the Puckorius scale, also indicating a tendency towards corrosion; LSkI appears not to be a suitable measure of corrosion in the areas sampled in Ethiopia, Malawi and Uganda, largely because of the ranges of alkalinity values observed

5.3 TRACE METALS FROM AQUIFER VS BOREHOLE AND HANDPUMP METALWORK

- pH and Eh plots suggest that the presence of dissolved Fe and Mn in most of the samples may be due to the aquifer conditions rather than necessarily indicating metal corrosion as the dominant control on dissolved concentrations
- It is tentatively suggested that Cr and Cu in Survey 1 samples may have a contribution from the borehole metalwork while Mn, Fe, Ni, Pb and Zn are inferred to be dominantly derived from the aquifers
- $SI_{calcite}$ and LSI indicate that most groundwaters in the database are undersaturated with respect to calcite, many significantly so

5.4 PH AS AN INDICATOR OF CORROSION RISK

The application of statistical models has shown that, for galvanised iron components:

- pH less than 6.5 is a good predictor of the probability of corrosion of galvanised iron rising mains and rods
- for galvanised iron rising mains, the corrosion probability is 61 % if pH is less than 6.5 and 30 % if pH is greater than 6.5; the equivalent probabilities for galvanised iron rods are 61 % and 50 %
- our results provide statistical validation of empirical measurements by Langenegger (1989, 1994) and good evidence for the continued use of pH of less than 6.5 as a simple and effective indicator of corrosion risk for galvanised iron components
- corrosion of components in groundwater above this threshold can still occur, but the probability is lower: when pH is above the thresholds (over 6.5) the likelihood of corrosion ranges from 30 to 50 %
- our results provide an indication of the probability of corrosion occurring, which allows planners and implementers to use more risk-based assessments of corrosivity for rural water infrastructure

The application of statistical models has shown that, for stainless steel components:

- based on our dataset and within our model, the probability of corrosion is 6.4 % if the pH is less than 7 and 50 % otherwise.
- corrosion of stainless steel rods was uncommon (only 40 rods from a sample of 534 displayed any evidence of corrosion) and results might have been influenced by confounding factors, interactions between variables or threshold artefacts
- although pH < 7 was identified as the most informative predictor within the model, the results suggest that pH alone is not a reliable predictor of stainless steel corrosion
- corrosion of stainless steel is governed by more complex mechanisms than the gradual dissolution of the Zn protective layer on galvanised iron:
    - stainless steel corrosion behaviour is controlled by the stability of a chromium oxide passive film
    - in groundwater systems, factors such as redox conditions, DO and Cl concentration are known to play a major role in passive film stability

6 Recommendations

Based on the findings of our work, we identify several recommendations, organised into three broad categories:

- how to decide what to measure and how that should be done
- what corrosion indicators should be used and how
- what to consider when making material choices and considering component replacement

6.1 WHAT TO ASSESS AND HOW TO EFFECTIVELY SAMPLE AND MEASURE

Different parameters provide different levels of information about the corrosion risk of groundwater. High-level screening using only pH can provide an indication of the probability of corrosion, but a comprehensive understanding of water chemistry is important when considering material selection or replacement. However, it is essential that sampling is carried out effectively for accurate results.

6.1.1 Water quality

A comprehensive analysis of water quality is warranted where budgets allow. This can provide important insights into the likelihood of corrosion of components and the impact of corrosion on water quality. This is also important prior to switching from galvanised iron to stainless steel where detailed, site-specific groundwater assessment is required at sites where pH is close to neutral or slightly acidic.

6.1.2 pH

Where reliance is placed on pH as an indicator, it is critical to be confident in the quality of the measurement. This should be supported by use of well maintained and regularly calibrated probes with fresh calibration solutions. Measurements should be allowed to stabilise before the value is recorded.

6.1.3 Survey design

Survey design is a very important component in investigations of groundwater quality and its controlling processes, so a robust design with good quality assurance is needed to reduce uncertainties:

- Onsite (field) measurements need to be carried out using reliable, maintained and calibrated meters and sensors with good-quality calibration solutions (pH; ORP; SEC). Readings should be allowed to stabilise before final measurements are recorded.
- Any corrections to field measurements should be made according to equipment manufacturers' instructions.
- Measurement of replicates, either in the field (for example, alkalinity; total Fe; turbidity) or in the laboratory, is essential to ensuring good data reproducibility.
- Collection of blanks is also important for laboratory analysis, as checks on sampling and equipment contamination.
- For exclusion of particulate metals from a water sample (such as needed in this study), fine filtration is necessary, preferably to a mesh of around 0.2 µm.
- Any reagents used for sample preservation (for example, strong acid) need to be sufficiently pure to negate contaminating samples to the extent of compromising the concentrations of analytes of interest.
- Repeat sampling benefits from the use of consistent sampling and analytical techniques and laboratories, facilitating consistent suites of analytes and detection limits.
- Care is needed to ensure adequate quality assurance procedures, including calculation of charge balances from major ions, with repeat analysis, if necessary, as well as attention to inconsistencies (such as differences between analyte concentrations by

different methods; coexistence of incompatible analytes such as dissolved O versus Fe or Mn; dissolved O versus H_2S).

6.1.4 Contaminant leaching

If the aim of an investigation is to assess leaching from hand pumps, groundwater samples should also be collected prior to pumping the borehole to ensure that results are indicative of leaching from pump components and not derived from the aquifer.

6.2 INDICATORS OF CORROSION RISK

Our analysis demonstrates that pH can be a good indicator of corrosion risk but that other indices can also be used to screen for the likelihood of corrosion.

- pH less than 6.5 is a good indicator of corrosion risk for galvanised iron components, but it is important to look at the overall water quality to obtain a better understanding of the corrosivity of groundwater.
- pH below 6.5 can be used as an indicator of corrosion for galvanised iron components where budgets are more limited; however, it is important to be aware that the risk of corrosion remains when using the pH indicator, even when components are installed in water with a pH above the threshold.
- pH is not a reliable indicator of corrosion risk for stainless steel; further research is required to establish what might serve as an effective indicator for stainless steel corrosion risk.
- Corrosion indices can be calculated from key field parameters and major ion water chemistry data. They provide a useful summary of the tendency of water to be corrosive. These indicators can provide a useful screening for likelihood of corrosion beyond the use of a simple pH threshold.

6.3 MATERIAL CHOICE AND REPLACEMENT

Our analysis reinforces more general principles about the use and replacement of materials in corrosive environments.

- In low-pH water, components (particularly metal components) need to be replaced regularly. The handpump manuals provide some guidance as to expected lifespans for individual components but, where groundwater has a tendency towards corrosion, regular monitoring of the components' condition is recommended.
- Use of appropriate materials may reduce, but does not eliminate, corrosion problems.
- Stainless steel is corrosion resistant and is increasingly being used. In Uganda, the use of galvanised iron has essentially been banned, and users are obliged to use stainless steel; however, stainless steel can be expensive, is generally not as widely accessible and needs to be of good quality.
- PVC or uPVC (for wells less than 45 m deep, but with ongoing trials in wells deeper than 45 m) are widely used in rising main pipes and do not corrode.
- Adherence to pump and metal manufacturing standards is crucial. Components, particularly rising mains and rods, should meet the standards laid out in the hand-pump manuals.

Appendix 1 Analytes in the Hidden Crisis database

Table A1 List of physicochemical and chemical analytes determined in surveys 1 and 2 of the Hidden Crisis project (coloured blue where analysed). Typical detection limits are given where comparisons apply.

Analyte	Units	Survey 1	Survey 2
Temperature	oC		
pH			
SEC	µS/cm		
Turbidity	NTU	some	some
Total Fe	mg/L	some	some
TTC	CFU/mL		
E. coli	mpn		
CDOM	µg/L		
TLF	µg/L		
NPOC	mg/L		
HCO_3	mg/L		
Eh	mV		
DO	mg/L		
F	mg/L		
Cl	mg/L		
Br	mg/L		
HPO_4	mg/L		
NO_3	mg/L		
NH_4	mg/L		
NO_2	mg/L		
SO_4	mg/L		
Ca	mg/L		
Mg	mg/L		
Na	mg/L		
K	mg/L		
S	mg/L		
Al	mg/L	0.05	
As	mg/L	0.05	
B	mg/L	0.05	
Cd	mg/L	0.05	
Co	mg/L	0.05	
Cr	mg/L	0.05	
Cu	mg/L	0.05	
Fe	mg/L	0.1	
Mn	mg/L	0.05	
Mo	mg/L	0.05	
Ni	mg/L	0.05	
P	mg/L	0.2	
Pb	mg/L	0.05	
Sb	mg/L	0.1	
Se	mg/L	0.05	
Si	mg/L		
Sr	mg/L	0.05	
Zn	mg/L	0.05	
Cr	µg/L	0.4	0.2
Mn	µg/L	0.4	0.5
Co	µg/L	0.4	0.08
Ni	µg/L	0.5	0.1
Cu	µg/L	0.5	0.4
Zn	µg/L	0.8	4
As	µg/L	0.2	0.04
Mo	µg/L	0.2	0.03
Cd	µg/L	0.2	0.02
Sb	µg/L	0.1	0.009
Pb	µg/L	0.05	0.02

Analyte	Units	Survey 1	Survey 2
Ba	µg/L		
Sr	µg/L		
Fe	µg/L		
Li	µg/L		
Be	µg/L		
B	µg/L		
Al	µg/L		
Ti	µg/L		
V	µg/L		
Ga	µg/L		
Se	µg/L		
Rb	µg/L		
Y	µg/L		
Zr	µg/L		
Nb	µg/L		
Ag	µg/L		
Sn	µg/L		
Cs	µg/L		
La	µg/L		
Ce	µg/L		
Pr	µg/L		
Nd	µg/L		
Sm	µg/L		
Eu	µg/L		
Gd	µg/L		
Tb	µg/L		
Dy	µg/L		
Ho	µg/L		
Er	µg/L		
Tm	µg/L		
Yb	µg/L		
Lu	µg/L		
Hf	µg/L		
Ta	µg/L		
W	µg/L		
Tl	µg/L		
Th	µg/L		
U	µg/L		
I	µg/L		

TTC: thermotolerant coliforms; CDOM: coloured dissolved organic matter; TLF: tryptophan-like fluorescence; NPOC: non-purgeable organic carbon; mpn: most probable number.

Appendix 2 Statistical parameters

INPUT VARIABLES

Table A2 Full set of input variables used in logistic regressions, with pre-normalisation units where present. Variables in italics are defined in sections 3.3 and 3.4, while all others are defined in UPGro (2020) and UPGro (2022). Variables in bold are used only for rising mains and rods.

log A	Cl (mg/L)	Zr_micro (µg/L)	U_micro (µg/L)	Sm_micro (µg/L)
T (°C)	SO_4 (mg/L)	Tl_micro (µg/L)	I_micro (µg/L)	Eu_micro (µg/L)
pH	NO_3 (mg/L)	Pb_micro (µg/L)	B_micro (µg/L)	Gd_micro (µg/L)
DO (mg/L)	Br (mg/L)	Th_micro (µg/L)	Al_micro (µg/L)	Tb_micro (µg/L)
Eh (mV)	NO_2 (mg/L)	Nb_micro (µg/L)	Ti_micro (µg/L)	Dy_micro (µg/L)
SEC (µS/cm)	HPO_4 (mg/L)	Mo_micro (µg/L)	V_micro (µg/L)	Ho_micro (µg/L)
Fe_field (mg/L)	F (mg/L)	Ag_micro (µg/L)	Cr_micro (µg/L)	Er_micro (µg/L)
TDS (mg/L)	NPOC (mg/L)	Cd_micro (µg/L)	Co_micro (µg/L)	*Calcite_saturation*
Ca (mg/L)	Ba_micro (µg/L)	Sn_micro (µg/L)	Ni_micro (µg/L)	*Langelier_index*
Mg (mg/L)	Sr_micro (µg/L)	Sb_micro (µg/L)	Cu_micro (µg/L)	*Ryznar_index*
Na (mg/L)	Mn_micro (µg/L)	Cs_micro (µg/L)	Zn_micro (µg/L)	*Puckorius_index*
TIC (mg/L)	Fe_micro (µg/L)	Tm_micro (µg/L)	Ga_micro (µg/L)	*LarsonSkold_index*
S (mg/L)	Li_micro (µg/L)	Yb_micro (µg/L)	As_micro (µg/L)	***Exposed***
NH_4 (mg/L)	Be_micro (µg/L)	Lu_micro (µg/L)	La_micro (µg/L)	***Immersed***
SiO_2 (mg/L)	Se_micro (µg/L)	Hf_micro (µg/L)	Ce_micro (µg/L)	***Min_water_depth*** *(m)*
K (mg/L)	Rb_micro (µg/L)	Ta_micro (µg/L)	Pr_micro (µg/L)	***GW_range*** *(m)*
HCO_3 (mg/L)	Y_micro (µg/L)	W_micro (µg/L)	Nd_micro (µg/L)	***Borehole_depth*** *(m)*

Table A3 List of conditions for binary indicator variables.

pH < 5.5	Calcite_saturation < 0
pH < 6.0	Langelier_index < 0
pH < 6.5	Ryznar_index > 7
pH < 7.0	Puckorius_index > 7
	LarsonSkold_index > 0.2

Table A4 Set of variables for which values in surveys 1 and 2 are compared to understand the effect of the pump on water chemistry.

pH	Cl	Mg	Cr_micro	As_micro	B_micro	Calcite_saturation
SEC	Br	Na	Mn_micro	Mo_micro	Fe_micro	Langelier_index
Turbidity	NO_3	S	Co_micro	Cd_micro	Se_micro	Ryznar_index
Fe_field	SO_4	P	Ni_micro	Sb_micro	Sr_micro	Puckorius_index
HCO_3	Ca	Si	Cu_micro	Pb_micro		LarsonSkold_index
F	K	TDS	Zn_micro	Al_micro		

Abbreviations

AGE	Above ground and external
AGI	Above ground and internal
BG	Below ground
BGS	British Geological Survey
BIC	Bayesian information criterion
CSIRO	Commonwealth Scientific and Industrial Research Organisation (Australia)
DO	Dissolved oxygen
Eh	Redox potential
ESRC	Economic and Social Research Council
FCDO	Foreign, Commonwealth & Development Office
IAP	Ion activity product
ICP-MS	Inductively coupled plasma mass spectrometry
ICP-OES	Inductively coupled plasma optical emission spectroscopy
LSI	Langelier saturation index
LSkI	Larson-Skold index
mbgl	Metres below ground level
NERC	Natural Environment Research Council
NTU	Nephelometric turbidity unit
ORP	Oxidation/reduction potential
pH	Potential of hydrogen: a quantitative measure of acidity/alkalinity
PHREEQC	A computer program for simulating chemical reactions and transport processes in natural or polluted water
PSI	Puckorius scaling index
PVC	Polyvinyl chloride
RSI	Ryznar stability index
SEC	Specific electrical conductivity
SI	Saturation index
SSA	Sub-Saharan Africa
TDS	Total dissolved solids
TIC	Total inorganic carbon
UKRI	UK Research and Innovation
WHO	World Health Organization

References

APHA. 2021. 1030 Data Quality. In *Standard Methods For The Examination Of Water And Wastewater.* Lipps, W, Baxter, T, and Braun-Howland, E (editors). (Washington DC: APHA Press.) Available: https://www.standardmethods.org/doi/10.2105/SMWW.2882.006

Banks, E W, Cook, P G, Owor, M, Okullo, J, Kebede, S, Nedaw, D, Mleta, P, Fallas, H, Gooddy, D, MacAllister, D J, Mkandawire, T, Makuluni, P, Shaba, C E, and MacDonald, A. M. 2021. Environmental tracers to evaluate groundwater residence times and water quality risk in shallow unconfined aquifers in sub-Saharan Africa. *Journal Of Hydrology*, Vol. 598, 125753. DOI: https://doi.org/10.1016/j.jhydrol.2020.125753

Benefield, L D, Judkins, J F, and Weand, B L. 1982. Process chemistry for water and wastewater treatment. (New Jersey, USA: Prentice-Hall.) ISBN: 978-0137229758

Bonsor, H, MacDonald, A, Casey, V, Carter, R, and Wilson, P. 2018. The need for a standard approach to assessing the functionality of rural community water supplies. *Hydrogeology Journal*, Vol. 26, 367–370. DOI: https://doi.org/10.1007/s10040-017-1711-0

Casey, V, Brown, L, Carpenter, J D, Nekesa, J, and Etti, B. 2016. The role of handpump corrosion in the contamination and failure of rural water supplies. *Waterlines*, Vol. 35, 59–77. DOI: https://doi.org/10.1007/s10040-017-1711-0

Clarke, F E. 1980. Corrosion and encrustation in water wells: a field guide for assessment, prediction and control. (Rome, Italy: Food and Agriculture Organization of the UN.) ISBN: 9251009333

Danert, K. 2022. Stop The Rot Report II: rapid corrosion of handpumps. Action Research On Handpump Component Quality And Corrosion In Sub-Saharan Africa. DOI: https://doi.org/10.13140/RG.2.2.34086.19528

Eslami, F, Salari, M, Yousefi, N, and Mahvi, A H. 2020. Evaluation of quality, scaling and corrosion potential of groundwater resources using stability index; case study Kerman Province (Iran). *Desalination And Water Treatment*, Vol. 179, 19–27. DOI: https://doi.org/10.5004/dwt.2020.24999

Fisher, M B, Guo, A Z, Tracy, J W, Prasad, S K, Cronk, R D, Browning, E G, Liang, K R, Kelly, E R, and Bartram, J K. 2021. Occurrence of lead and other toxic metals derived from drinking-water systems in three West African countries. *Environmental Health Perspectives*, Vol. 129, 047012. DOI: https://doi.org/10.1289/ehp7804

Hastie, T, Tibshirani, R, and Friedman, J H. 2009. The elements of statistical learning: data mining, inference, and prediction. (Springer.) DOI: https://doi.org/10.1007/b94608

Kinniburgh, D G, and Cooper, D M. 2004. Predominance and mineral stability diagrams revisited. *Environmental Science & Technology*, Vol. 38(13), 3641–3648. DOI: https://doi.org/10.1021/es034927l

Langenegger, O. 1989. Groundwater quality - an important factor for selecting handpumps. *Developments In Water Science*, Vol. 39, 531–541. DOI: https://doi.org/10.1016/S0167-5648(08)70561-6

Langenegger, O. 1994. Groundwater quality and handpump corrosion in Africa. *Water and Sanitation Program Report.* (Washington, D.C.: UNDP-World Bank Water and Sanitation Program.)

Lapworth, D J, MacDonald, A M, Kebede, S, Owor, M, Chavula, G, Fallas, H, Wilson, P, Ward, J S T, Lark, M, Okullo, J, Mwathunga, E, Banda, S, Gwengweya, G, Nedaw, D, Jumbo, S, Banks, E, Cook, P, and Casey, V. 2020. Drinking water quality from rural handpump-boreholes in Africa. *Environmental Research Letters*, Vol. 15, 064020. DOI: https://doi.org/10.1088/1748-9326%2Fab8031

Ma, F-Y 2012. Corrosive effects of chlorides on metals. 139–178 in *Pitting Corrosion*. Bensalah, N (editor). DOI: https://doi.org/10.5772/32333

MacAllister, D J, Nedaw, D, Kebede, S, Mkandawire, T, Makuluni, P, Shaba, C, Okullo, J, Owor, M, Carter, R, Chilton, J, Casey, V, Fallas, H, and MacDonald, A M. 2022. Contribution of physical factors to handpump borehole functionality in Africa. *Science Of The Total Environment*, Vol. 851, 158343. DOI: https://doi.org/10.1016/j.scitotenv.2022.158343

MacAllister, D J, Whaley, L, Gurmessa, S K, Nedaw, D, Tadesse, Y, Mwathunga, E, Mkandawire, T, Makuluni, P, Shaba, C, Banda, S, Owor, M M, Okullo, J, Katusiime, F, Carter, R, Chilton, J, Casey, V, Fallas, H, Cleaver, F, and MacDonald, A M. 2026. Connecting narratives and numbers to investigate the interaction of social, physical and technical determinants of rural water supply performance. *PLOS Water*, Vol. 5, E0000486. DOI: https://doi.org/10.1371/journal.pwat.0000486

Mankikar, T Y. 2021. Comparison of indices for scaling and corrosion tendency of groundwater: case study of unconfined aquifer from Mahoba District, U.P. State. *Applied Water Science*, Vol. 11, 94. DOI: https://doi.org/10.1007/s13201-021-01423-3

Parkhurst, D L, and Appelo, C A J. 2013. Description of input and examples for PHREEQC version 3—a computer program for speciation, batch-reaction, one-dimensional transport, and inverse geochemical calculations. Chapter 43 of Section A: Groundwater in *Book 6 Modeling Techniques*. DOI: https://doi.org/10.3133/tm6A43

Rezek, K, Fisher, M, Purvis, T, Salzberg, A, Minyila, S, and Roy, S. 2026. Quantifying lead (Pb) leaching from galvanized handpump spouts, leaded brass taps, and stainless-steel alternatives using the NSF 61 test protocol: implications for safe rural water supply. *PLOS Water*, Vol. 5(4), E0000402. DOI: https://doi.org/10.1371/journal.pwat.0000402

Roberge, P R. 2007. Corrosion Inspection And Monitoring. (John Wiley & Sons.) DOI: http://doi.org/10.1002/0470099763

Robinson, A L. 2024. Potential corrosivity of untreated groundwater in Louisiana. *Scientific Investigations Report* 2024-5035. (US Geological Survey.) DOI: https://doi.org/10.3133/sir20245035

UPGro 2020. Hidden Crisis Project, Survey 2 dataset: hand pump borehole diagnostic tests in Ethiopia, Uganda And Malawi. (British Geological Survey.) DOI: https://dx.doi.org/10.5285/cdbca137-0bb3-4281-b872-399a4df8e946

UPGro 2022. Hidden Crisis Project, Survey 1 dataset: detailed functionality assessments of hand pump boreholes in Ethiopia, Uganda And Malawi. (British Geological Survey.) DOI: https://dx.doi.org/10.5285/bca0d930-a10d-4ae8-9afc-ad1bf73de35a

World Bank. 2024. Preventing rapid corrosion of handpumps through regulations. In *Water Knowledge Note.* Kerstin Danert, S F (editor). (Washington DC: World Bank Group.) Availale: http://documents.worldbank.org/curated/en/099052424151038179

World Health Organization. 2022. Guidelines For Drinking-Water Quality: fourth edition incorporating first and second addenda. (World Health Organization.) ISBN: 978-92-4-004506-4